The influence of sediment thermal maturity and hydrocarbon formation on Hg behaviour in the stratigraphic record

Asri Oktavioni Indraswari[1], Joost Frieling[1], Tamsin A. Mather[1], Alexander Dickson[2], Hugh Jenkyns[3], and Erdem Idiz[1]

[1]University of Oxford
[2]Royal Holloway University of London
[3]Oxford University

December 7, 2022

Abstract

While Hg in sediments is increasingly used as a proxy for deep-time volcanic activity, the behaviour of Hg in OM-rich sediments as they undergo thermal maturation is not well understood. In this study, we evaluate the effects of thermal maturation on sedimentary Hg contents and, thereby, the impact of thermal maturity on the use of the Hg/TOC proxy for large igneous province (LIP) volcanism. We investigate three cores (marine organic matter) with different levels of thermal maturity in lowermost Toarcian sediments (Posidonienschiefer) from the Lower Saxony Basin in Germany. We present Hg content, bulk organic geochemistry, and total sulfur in three cores with different levels of thermal maturity. The comparison of Hg data between the three cores indicates that Hg content in the mature/overmature sediments have increased > 2-fold compared to Hg in the immature deposits. Although difficult to confirm with the present data, we speculate that redistribution within the sedimentary sequence caused by the mobility and volatility of the element under relatively high temperatures may have contributed to Hg enrichment in distinct stratigraphic levels of the mature cores. Regardless of the exact mechanism, elevated Hg content together with organic-carbon loss by thermal maturation exaggerate the value of Hg/TOC in mature sediments, suggesting that thermal effects have to be considered when using TOC-normalised Hg as a proxy for far-field volcanic activity.

The influence of sediment thermal maturity and hydrocarbon formation on Hg behaviour in the stratigraphic record

A. O. Indraswari[1,2], J. Frieling[1], T. A. Mather[1], A. J. Dickson[3], H. C. Jenkyns[1], E. Idiz[1]

[1]Department of Earth Sciences, University of Oxford, South Parks Road, Oxford, OX1 3AN, UK.

[2]Geoscience Study Program, Faculty of Mathematics and Natural Sciences (FMIPA), Universitas Indonesia, Depok 16424, Indonesia.

[3]Centre of Climate, Ocean and Atmosphere, Department of Earth Sciences, Royal Holloway University of London, Egham, Surrey, TW20 0EX, UK.

Corresponding author: Asri O. Indraswari (asri.indraswari@exeter.ox.ac.uk)

Key Points:

- Thermal maturation of organic-rich deposits has increased Hg content > 2-fold
- Hg/TOC ratios from mature sediments are inflated because of organic carbon loss from the host rock during maturation
- Thermal history of sediments must be considered when using Hg as a proxy for volcanism

Abstract

While Hg in sediments is increasingly used as a proxy for deep-time volcanic activity, the behaviour of Hg in OM-rich sediments as they undergo thermal maturation is not well understood. In this study, we evaluate the effects of thermal maturation on sedimentary Hg contents and, thereby, the impact of thermal maturity on the use of the Hg/TOC proxy for large igneous province (LIP) volcanism. We investigate three cores (marine organic matter) with different levels of thermal maturity in lowermost Toarcian sediments (Posidonienschiefer) from the Lower Saxony Basin in Germany. We present Hg content, bulk organic geochemistry, and total sulfur in three cores with different levels of thermal maturity. The comparison of Hg data between the three cores indicates that Hg content in the mature/overmature sediments have increased $>$ 2-fold compared to Hg in the immature deposits. Although difficult to confirm with the present data, we speculate that redistribution within the sedimentary sequence caused by the mobility and volatility of the element under relatively high temperatures may have contributed to Hg enrichment in distinct stratigraphic levels of the mature cores. Regardless of the exact mechanism, elevated Hg content together with organic-carbon loss by thermal maturation exaggerate the value of Hg/TOC in mature sediments, suggesting that thermal effects have to be considered when using TOC-normalised Hg as a proxy for far-field volcanic activity.

1. Introduction

Mercury (Hg) is highly toxic, which means that understanding its behaviour in shallow- and deep-earth environments and how it cycles through ecosystems is of considerable importance. Emissions of Hg into the atmosphere include those from natural sources, such as volcanic exhalations, and anthropogenic sources, such as artisanal and small-scale mining, fossil-fuel combustion, non-ferrous metal smelting, and cement production (UN Environment, 2019). Critically, a substantial part of these emissions is in gaseous form, and the relatively long atmospheric lifetime of Hg (0.5–2 years) means that it can be globally dispersed before deposition (e.g., Lindqvist et al., 1991; Mason et al., 1994; Lamborg et al., 2002a,b). It is generally assumed that most of the Hg will be finally sequestered in sediments containing organic matter (OM) as OM-Hg complexes. Indeed, field-data show that OM is usually the dominant Hg carrier, both in the water column and sediment (Wallace, 1982; Benoit et al., 2001; Outridge et al., 2007). In addition to OM, sulfides (e.g., HgS and Hg-inclusions in pyrite) and clays may prove significant sedimentary Hg hosts (Percival et al., 2018; Shen et al., 2020; Wang et al., 2020).

The behaviour of Hg once deposited into sedimentary archives is of interest for several reasons. The presence and levels of Hg in oils and their organic-rich petroleum source rocks is important as it is considered a contaminant in hydrocarbon fields. Mercury is found in hydrocarbons in highly varying concentrations (Wilhelm & Bloom, 2000). For example, fuel oils contain Hg with values ranging from 7 to 30,000 ppb, with a typical value being 3500 ppb (Wilhelm, 2001; Mukherjee et al., 2009). Knowledge about the presence and level of Hg in these hydrocarbon streams is essential because it can determine, amongst other things, decisions regarding processing facility design (e.g., the inclusion of costly removal units) to mitigate Hg pollution (Wilhelm & Bloom, 2000; Gajdosechova et al., 2016). The observed variable and potentially very high Hg content in hydrocarbons implies that it is critical to understand which sedimentary strata are likely to be enriched in Hg during deposition, and what processes might move and concentrate Hg into expelled fluids during thermal maturation of sediments.

Further to concerns regarding Hg behaviour in hydrocarbons, there has been much recent interest in the potential of Hg as a proxy for large-scale volcanism (namely large igneous provinces (LIP)) in the sedimentary record since volcanoes are amongst the largest natural sources (Pyle & Mather, 2003; Sanei et al., 2012; Percival et al., 2015; Scaife et al., 2017; Percival et al., 2021). Hg records are usually normalised to Total Organic Carbon (TOC) to correct for increases in Hg content associated with greater TOC contents (Sanei et al., 2012; Grasby et al., 2019). However, Hg can also be bound to sulfides and clay minerals and, in some environments, Hg deposition with such geochemical species may confound the usual sedimentary Hg-OM relationship (see e.g., Sanei et al., 2012; Charbonnier & Föllmi, 2017; Percival et al., 2018). Thus, several works (e.g., Grasby et al. (2019) and Shen et al. (2020)) have argued that it is critical to look at the

relationship of Hg with TOC, as well as Hg variance with clay (Al) and total sulfur levels. Moreover, several previous studies acknowledge the potential of changes to geological deep-time sedimentary Hg records induced by OM sources or types that, for example, may be related to coastal proximity (i.e., marine- *vs* terrestrial-derived OM; Grasby et al., 2017; Wang et al., 2018; Them et al., 2019). Various fixation mechanisms for Hg in organic-rich mudrocks have been investigated, including adsorption onto OM and clay minerals and incorporation of Hg into the crystal structures of other host minerals, particularly sulfides (Krupp, 1988; Shen et al., 2020). Pyrite-hosted Hg might become a more dominant phase when sediments are deposited under sulfidic conditions, where free H_2S occurs in the water column or sediment pore waters (Shen et al. 2020). However, whether these factors also lead to enhanced Hg sequestration or how these conditions affect proportioning between sedimentary host phases is not well constrained. While various potential confounding factors on sedimentary Hg distributions have been investigated (Grasby et al., 2019; Shen et al., 2020), the effects of thermal maturity on Hg content in deep-time sediments have not been tested systemically. This is however a critical knowledge gap as sedimentary Hg can be mobilised at temperatures known to be relevant for post-depositional sediment alteration and resulting oil and gas generation (e.g., Rumayor et al., 2013; Liu et al., 2022) and is clearly enriched in some hydrocarbon sources (e.g., Wilhelm, 2001; Mukherjee et al., 2009).

Thermal maturation of labile sedimentary OM occurs due to increasing temperature with increasing burial depth, typically on the order of ˜30°C rise in temperature per kilometre of overburden. in catagenesis, that is conversion of kerogen, stable at lower temperatures, through thermal cracking into lower molecular weight components, loosely defined as bitumen. In the early stage of maturation, this bitumen contains a large proportion of high-molecular-weight compounds such as resins and asphaltenes. With increasing maturation, bitumen undergoes further cracking and disproportionation, resulting in lower molecular-weight hydrocarbon molecules and an insoluble coke-like C-rich residue: pyrobitumen (Tissot & Welte, 1984; Sanei, 2020). As the kerogen becomes more thermally 'mature' it progresses through the stages of oil and gas generation and, depending on the type of kerogen, potentially loses up to 60% of its organic matter mass due to migration of the generated products away from the host rock (Lewan et al., 1979; Tissot & Welte, 1984; Raiswell & Berner, 1987).

Thermal maturation may play a key role in altering the geochemical signature of metals (e.g., Mo, V, and Ni) due to the close association of these geochemical species with sedimentary OM and the transformations that OM undergoes (Lewan & Maynard, 1982; Chappaz et al., 2014; Dahl et al., 2017). For example, thermal maturation has been shown to lead to progressive enrichment in both the concentration of metals and their TOC-normalised values in sedimentary rocks for Mo, Zn, U and Cd (Dickson et al., 2020, 2022). Such increases can be attributed to the loss of mass caused by the removal of bitumen during thermal maturation and the minor partitioning of metals into mobilized organic fluid phases (Dickson et al., 2020, 2022). The generation of H_2O, CO_2, and H_2S from both the organic and inorganic phases in the rocks also might play a role in causing additional mass losses (Abarghani et al., 2020; Dickson et al., 2020). However, it is difficult to directly measure metals bound to kerogen since the primary method to isolate this organic component is by digesting the mineral matrix using strong acids such as HF and HCl, which can also leach metals from the kerogen itself. Therefore, the mechanistic behaviour of metals, including Hg, in OM-rich sediments as they undergo thermal maturation is still not well understood.

Unlike most metals, there is evidence from analytical methods that utilise thermal desorption that sediments exposed to temperatures during burial typical of sedimentary basins (60–225 °C) could mobilise some Hg compounds (e.g., elemental Hg, weakly absorbed Hg, Hg-halides) (Rumayor et al., 2013, Liu et al. 2022), but the combined effects of prolonged exposure to the pressure and temperature regimes that typically exist during maturation remain untested.

Our study explores the influence of thermal maturation on sedimentary Hg using three cores covering a wide range of thermal maturity from the Lower Saxony Basin, Germany. By investigating Hg, bulk OM characteristics and total sulfur contents in a stratigraphically constrained interval from a single basin, we examined the role of thermal maturation as a key factor in post-depositional Hg mobility in sediments.

We focus on the part of the Posidonienschiefer that stratigraphically sits above the negative carbon-isotope excursion characteristic of the Toarcian Oceanic Anoxic Event (T-OAE).

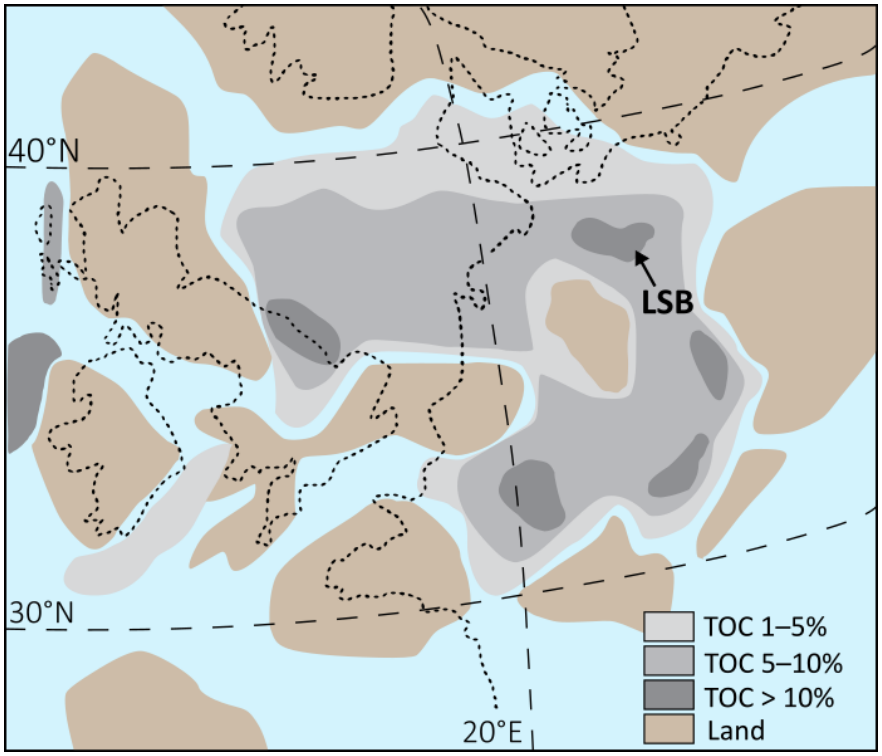

Figure 1. Location of the Lower Saxony Basin (LSB) in the Early Jurassic (ca. 182 Ma). Modern shorelines are shown as dashed lines. TOC—total organic carbon.

Geological Setting

The Lower Saxony Basin (LSB), located in north-western Germany (Fig. 1), is the country's most important oil province (Betz et al., 1987). It is a 300-km long and 65-km wide E–W-oriented basin formed during the breakup of the supercontinent Pangaea through extension and subsidence (Betz et al., 1987; Brink et al., 1992; Bruns et al., 2013). The Lower Toarcian Posidonienschiefer is a distinct organic-rich unit preserved in the LSB. For more than a century, this unit has been of scientific interest due to its importance as a source rock, including sedimentology (Littke et al., 1991; Röhl et al., 2001; Schmid-Röhl et al., 2002), stratigraphy (Riegraf et al., 1984; Frimmel et al., 2004; Schwark & Frimmel, 2004), petrology and geochemistry (Jenkyns, 1985, 1988; Leythaeuser et al., 1988; Rullkötter et al., 1988; Rullkötter & Marzi, 1988; Littke et al., 1988, 1991; Wilkes et al., 1998).

Evidence of persistent euxinia in the water column, and specifically indicators of free H_2S in the photic zone, comes from the identification of aryl isoprenoids and other carotenoids (isorenieratene) reported in the Posidonienschiefer from the LSB (Blumenberg et al., 2019) and from the Posidonia shales from other NW European basins (Schwark & Frimmel, 2004; French et al., 2014; Song et al., 2017). Redox conditions are important to consider when interpreting the variability of Hg records, which may result in enhanced Hg or subdued Hg sequestration and/or changes in sedimentary host-phase (e.g., Grasby et al., 2016; Them et al., 2019, Shen et al., 2019; Grasby et al., 2019; Frieling et al., 2022 PREPRINT). However, since the Posidonienschiefer was likely deposited under basin-wide euxinic conditions (Blumenberg et al., 2019), we do not expect differences in the Hg sequestration pathway between the analysed core localities. Because of high marine productivity and relatively minor influences of terrestrial OM (Rullkötter et al., 1988; Littke

et al., 1991), major differences in OM-type between cores are also unlikely, excluding influences of variable proportions of marine and terrestrial OM on Hg loading.

Since its deposition in the Early Jurassic the Posidonienschiefer has been buried to various depths within the LSB, due to the effect of locally variable fault-bounded basin subsidence, followed by basin inversion during the Paleogene (Betz et al., 1987). As a result, the thermal maturity of the OM contained within the Posidonienschiefer varies over relatively short horizontal distances of tens of kilometres, making it a good candidate for testing whether thermal maturation can change the concentration of metals in organic-rich sedimentary rocks (Dickson et al., 2022).

Three ˜30-m-long drilled cores containing stratigraphically equivalent sections of the Posidonienschiefer were retrieved from different parts of the LSB. Two of the cores (core A and B) have been studied previously to explore the maturation-dependent changes in stable-isotope compositions and concentrations of Mo, Zn, Cd and U (Dickson et al., 2020, 2022) and the growth of the bed-parallel and oblique calcite veins known as 'beef' (Hooker et al., 2020). The thermal maturity of each core was established by reflectance measurements (%Ro) on terrestrial organic macerals (vitrinite˜0.5% for core A (immature) and ˜1.5% and ˜3.5% (post-mature) for core B and core C, respectively. Because cores B and C lack a biostratigraphic framework, a core-to-core correlation is achieved via distinct basin-wide chemostratigraphic trends in the TOC and trace-metal records. Using the $\delta^{13}C_{org}$ data for core A and subsequent correlation using the TOC of all three cores, we identify the interval of the Posidienschiefer that was deposited after the T-OAE, to avoid the Hg-cycle perturbation that characterises the T-OAE (Percival et al., 2015; Fantasia et al., 2018; Them et al., 2019).

3. Methods

A total of 647 samples (478 for core A, 121 for core B, and 48 for core C, with a stratigraphic resolution of 10 to 30 cm) were powdered and analysed for Hg content. Mercury content was measured on a Lumex RA-915 Portable Mercury Analyser coupled to a PYRO-915 pyrolysis unit at the University of Oxford (Bin et al., 2001). Powdered samples of between 50 and 100 mg were introduced into a sample boat, heated to >700 °C and left for up to 120 seconds to fully volatilize the Hg present. The instrument was calibrated before each run using NIST-SRM2587 (National Institute of Standards and Technology – Standard Reference Material: Trace Elements in Soil Containing Lead from Paint), with a Hg content of 290 ppb. The same standard was run for every ten samples to correct instrument drift. We calculate an external reproducibility of +-8.7% based on the repeat standard measurements (1 standard deviation (S.D.), n=199).

Hydrogen and oxygen indices (HI, OI) and TOC content data of all three cores have been published previously in Hooker et al. (2020). An additional 39 new samples (15 for core A, 21 for core B, and 3 for core C) were analysed with a Rock-Eval 6, following the methods in Behar et al. (2001), at the University of Oxford. The in-house standard SAB134 (Blue Lias organic-rich marl, 2.74 % TOC) was measured every 8 to 10 samples. The standard deviation of the in-house standard (SAB134) was ˜0.03 % TOC (1 S.D.).

Analyses of total sedimentary sulfur (%TS) were undertaken on 155 samples (57 for core A, 50 for core B, and 48 for core C). An aliquot of each sample was wrapped in a tin capsule and then combusted using an Elemental Cube Elemental Analyzer Vario El III at the Department of Earth Sciences, Royal Holloway University of London (Carvajal-Ortiz et al., 2021; Fadeeva et al., 2008). A sulfanilamide reference standard (18.62 % S) was analysed at the start and end of each run and between every ten samples to monitor instrument drift. Within-run reproducibility calculated from the Eocene shale standards (1.24 % S) run as unknowns was +-0.12 % S (1 S.D., n=12).

High-resolution $\delta^{13}C_{org}$ data from core A was measured by Celestino (2019). $\delta^{13}C_{org}$ for core B and core C were analysed at the Open University (U.K). The samples powders were prepared by decarbonating bulk sediments in 1M HCl before rinsing with de-ionised water until a neutral pH was reached. Samples were dried and re-powdered before being weighed into tin capsules and analysed using a Thermo MAT253 mass spectrometer coupled to a Flash HT combustion system. $\delta^{13}C_{org}$ is expressed relative to the Vienna Pee Dee Belemnite (VPDB) scale via within-run calibration using NIST 8572 glutamic acid (-26.39 (IAEA) CH-6 sucrose (-10.45 precision, calculated from the 1 S.D. of L-alanine, is better than ±0.1

4. Results

We focus on an interval of Posidonienschiefer that is stratigraphically above the negative carbon-isotope excursion characteristic of T-OAE (hereafter referred to as Posidonienschiefer). The stratigraphic successions of the cores in this study were tied together based on distinctive patterns in total organic carbon (TOC) following Dickson et al. (2022). The average TOC values of the Posidonienschiefer show an increase from core A to core B and from core B to core C (Table 1). Rock-Eval determined Hydrogen Index (HI) values in the section in core A average 687 mg hydrocarbons /g TOC (Fig. 2). By contrast, in cores B and C, the HI values throughout the Posidonienschiefer are relatively constant at near 0 (Fig. 3 and 4). Total sulfur (TS) content is ranging from 1.5 to 6 % for cores A, B, and C through the Posidonienschiefer, (Fig. 2, 3, and 4).

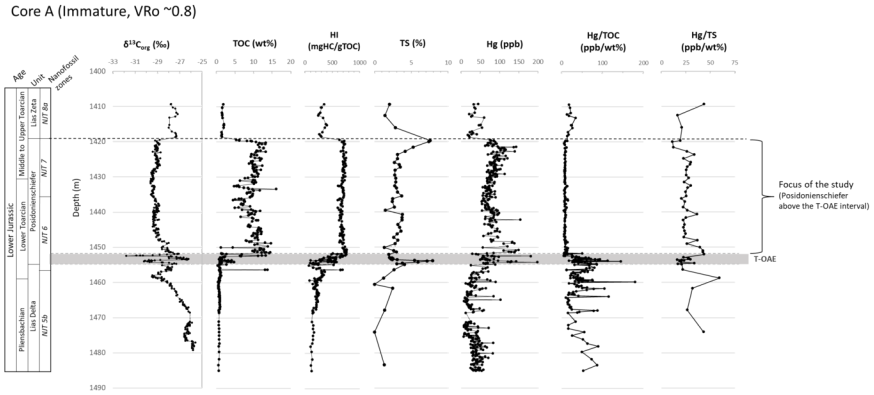

Figure 2 . Stratigraphic log of the studied core A (immature, VRo ˜0.8) showing $\delta^{13}C$ data from bulk OM, the total organic carbon (TOC), hydrogen index (HI), total sulfur (TS), Hg content, Hg normalised by TOC, and Hg normalised by TS.

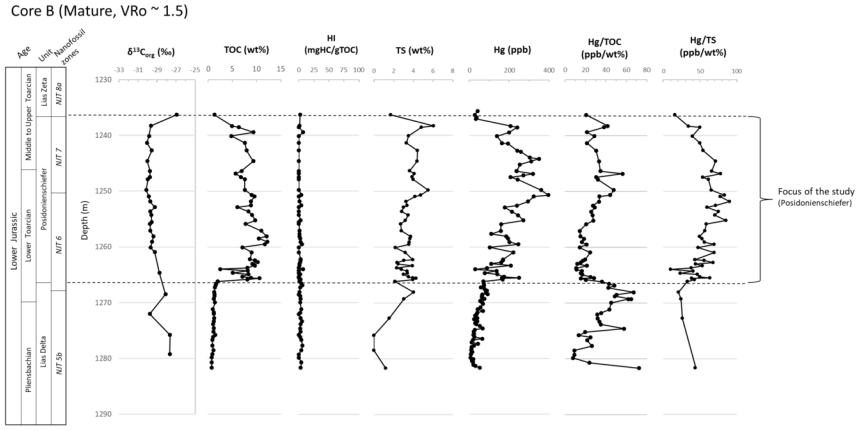

Figure 3 . Stratigraphic log of the studied core B (mature, VRo ˜1.5) showing $\delta^{13}C$ data from bulk OM, the total organic carbon (TOC), hydrogen index (HI), total sulfur (TS), Hg content, Hg normalised by TOC, and Hg normalised by TS.

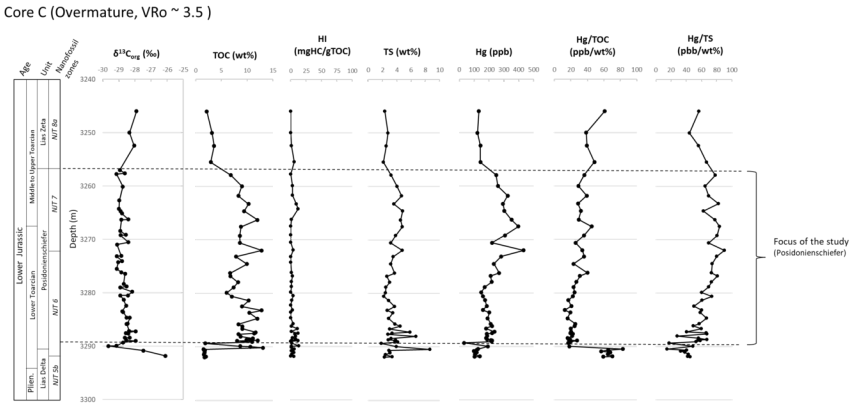

Figure 4 . Stratigraphic log of the studied core C (overmature, VRo ˜3.5) showing $\delta^{13}C$ data from bulk OM, the total organic carbon (TOC), hydrogen index (HI), total sulfur (TS), Hg content, Hg normalised by TOC, and Hg normalised by TS.

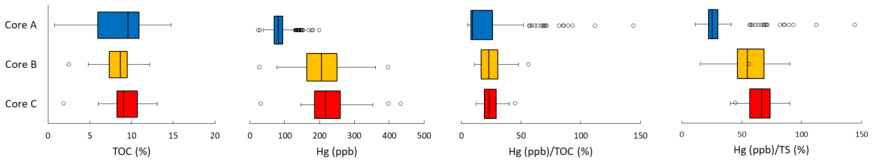

Figure 5 . Differences between cores A, B and C in the mean (vertical lines), interquartile range (boxes) and data within 1.5 interquartile range (black lines with bar ends) of TOC (%), Hg (ppb), Hg/TOC (ppb/%), and Hg/TS (ppb/%) in the Posidonienschiefer.

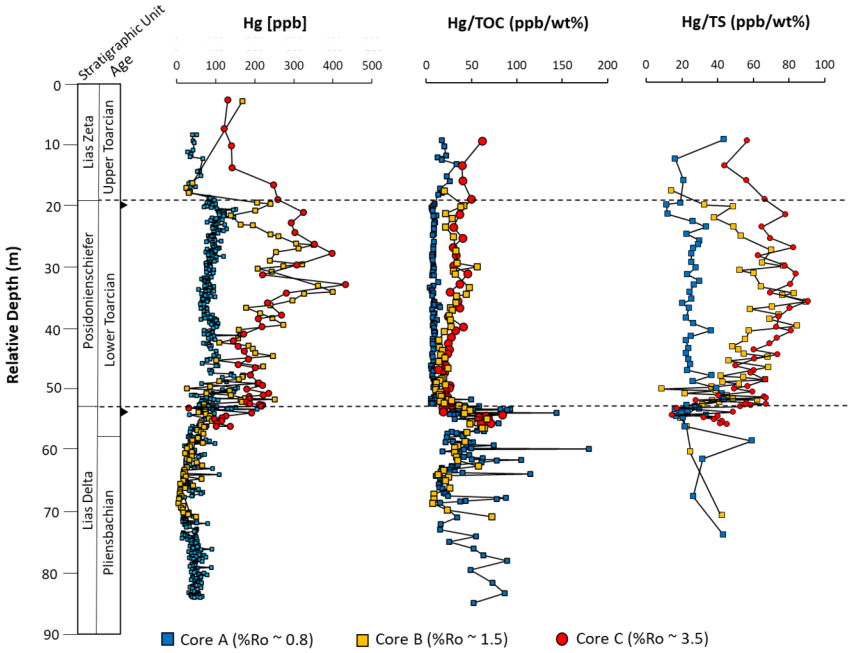

Figure 6. Hg contents, Hg/TOC, and Hg/TS in cores A, B, and C.

Table 1. TOC, Hg, TS, HI, OI and trace-metal data for cores A, B and C from the Posidonienschiefer. Symbols $^{+}$indicate data from Hooker et al. (2020) and * from Dickson et al. (2022).

		Core	Core	Core
		A	B	C
TOC	Mean	7.74	8.32	8.99
(%)	Std. Dev.	4.13	2.03	2.49
Hg	Mean	87.56	202.98	225.13
(ppb)	Std. Dev.	29.13	75.62	74.5
TS	Mean	3.47	3.59	3.73
(%)	Std. Dev.	1.5	0.82	1.28
Hydrogen Index^{+}	Mean	589	2	3
(mgHC/gTOC)	Std. Dev.	155	2	4
Oxygen Index^{+}	Mean	21	19	13
($mgCO_2$/gTOC)	Std. Dev.	36	11	4
Cd*	Mean	1.7		1.8
(ppm)	Std. Dev.	1.1		0.6
Zn*	Mean	178		217
(ppm)	Std. Dev.	97		80
U*	Mean	5.7		16.1
(ppm)	Std. Dev.	2.4		11.8
Mo*	Mean	70.45		101.9
(ppm)	Std. Dev.	39.9		52.3

Table 2. Correlation between Hg, TOC, and TS for cores A, B and C from the Posidonienschiefer.

		Core	Core	Core
		A	B	C
Hg-TOC	N	166	42	38
	R	0.309	0.254	0.427
	R^2	0.096	0.065	0.182
	p	<0.001	0.052	0.004
Hg-TS	N	48	41	38
	R	0.651	0.607	0.289
	R^2	0.424	0.368	0.084
	p	<0.001	<0.001	**0.039**
TS-TOC	N	48	41	38
	R	-0.086	-0.111	-0.07
	R^2	0.007	0.012	0.005
	p	0.28	0.246	0.338

Within the Posidonienschiefer, Hg content fluctuates between 53–154 ppb in core A (Fig. 2). In the equivalent interval of cores B and C, the range of Hg content is 28–397 ppb (Fig. 3) and 32–433 ppb (Fig. 4) respectively. The mean Hg content increases from 85 ppb (core A) to 203 ppb (B) and 225 ppb (C) (Table 1, Fig. 5). The Hg/TOC ratio in core A is in the range of 5–20 ppb/%, 10–56 ppb/% in core B, and 12–83 ppb/% in core C. The T-OAE-associated negative CIE is not clearly identifiable in cores B and C.

In core A, Hg/TOC ratios are very stable below 10 ppb/% throughout the Posidonienschiefer (Fig. 2), while in core B and core C, the Hg/TOC values fluctuate more (Fig. 2, 3, and 4). The Hg/TOC ratios in core A diverge from those for cores B and C (Fig. 6). Above 50 m relative depth core A Hg/TOC is persistently lower (˜10 ppb/%) compared to ˜20 to 50 ppb/% for cores B and C. The Hg/TS ratio in core A is relatively stable throughout the Posidonienschiefer. Similar to the Hg/TOC signal, the Hg/TS signal in cores B and C diverges above 50 m relative depth from the core A Hg/TS signal (Fig. 6). The Hg/TS in cores B and C shows an increasing trend in the lower to the middle part of the section (max ˜80-90 ppb/S%). The signal stabilises toward the top of the Posidonienschiefer in core B but decreases to 10 ppb/S% in core C (Fig. 6).

Correlations between Hg, TOC, and TS in the main high TOC sections are presented in Table 2. All individual correlations between Hg, TOC and TS explain less than 50% (R^2 <0.5) of the observed variance. With the exception of core B, Hg shows weak but significant (p <0.01) correlations with TOC. A similar relationship is found for TS, and Hg correlates significantly to TS in all cores. For core A and core B, Hg has stronger correlations with TS than with TOC. By contrast, Hg shows a very weak correlation with TS in core C and a weak correlation with TOC.

5. Discussion

5.1. Organic-matter characteristic of the Posidonienschiefer

In all three cores, Hg content in the Posidonienschiefer are higher than in the underlying Lias Zeta and overlying Lias Delta (Fig. 2, 3, and 4). The increased Hg content appear coincident with the much higher TOC in the Posidonienschiefer, a marked change from the marls and carbonate-dominated lithologies stratigraphically above and below, differences that reflect very pronounced changes in depositional redox conditions (Dickson et al., 2022). Within the Posidonienschiefer, the highest average TOC content is found in core C, followed by core B and core A (Table 1). This pattern is most likely a function of higher initial OM content in cores B and C, which, in turn, could be the result of their more distal position of the cores relative to the palaeo-shoreline (Dickson et al., 2022) and subdued siliciclastic input relative to supply of organic matter.

With HI values around 650–750 and oxygen index (OI) values under 20, the Posidonienschiefer can be interpreted as Type I/II kerogen showing a primary algal and amorphous organic-matter-dominated maceral assemblage (Littke et al., 1991). Algal-OM has shown high rates of Hg scavenging in modern lake and marine environments (Wallace, 1982; Zaferani et al., 2018; Outridge et al., 2019). Combined with the elevated TOC values (˜5–15%), this interval can be identified as an excellent oil/gas-prone source-rock. Such sediments would undergo TOC breakdown when reaching burial temperature (50–150 °C), which, in turn, might affect Hg content and consequently Hg/TOC after the thermal maturation.

The stable TOC, HI and OI values within the Posidonienschiefer itself suggest only minor changes in the OM type, making the Posidonienschiefer ideal for studying the effects of thermal maturation on Hg contents and normalised Hg. In contrast to core A, HI and OI values throughout cores B and C are extremely low throughout, consistent with the highly mature to post-mature stages of catagenesis experienced by the latter two cores (Tissot & Welte, 1984).

5.2. Mercury enrichment, carrier-phase depletion, or mobilisation in mature sediment?

We find that the average Hg content in the Posidonienschiefer is much higher in core B and core C compared to core A (Table 1, Fig. 5, 6). For the Posidonienschiefer, cores B and C have, on average, ˜2.3–2.6-fold higher Hg content than core A. Assuming OM and sulfides were the dominant Hg carriers at the time of deposition, the elevated TOC influenced by the relative position of each core within the basin (see discussion §5.1) may have caused higher original Hg content in immature cores B and C. As can be seen in the divergent Hg and TOC- and S-normalised Hg, the most common carrier phases for Hg show a different signal compared to the element itself (Fig 6).

It is not possible to know exactly how much of the original organic-carbon content of the sediments has been lost during maturation. However, in an extreme scenario, up to ca. 60% of the original organic-carbon content of the sediments may have been lost during maturation (Lewan et al., 1979; Tissot & Welte, 1984; Raiswell &

Berner, 1987). In turn, loss of organic carbon may have resulted in a significant (relative) enrichment in trace elements, if these were retained in the host rock. Hydrocarbon expulsion from the more mature cores thus potentially would have increased the relative trace-element concentrations through loss of mass. In addition to TOC loss, the removal water from the dehydration of clays during heating also likely contributed to the loss of rock mass (Peters & Cassa, 1994). A significant TOC loss will manifestly cause a more elevated value of normalised Hg/TOC in high-maturity OM-rich rocks (Fig. 5 and 6) if Hg is retained. This potentially results in a bias in both measured Hg and normalised Hg relative to the original signal stored in the rock record.

To assess whether mass loss or hydrocarbon expulsion processes have influenced the composition of our core material we compare our Hg data to previously published trace-element data. If the process of metal concentration due to loss of OM and water played a dominant role, the magnitude of change in Hg should resemble the relative increase in other (immobile) trace elements such as Mo, Zn, and Cd. Trace-metal increases observed between core A and core C did not exceed +45%, except for U (+185%; Table 1) (Dickson et al., 2020, 2022). The increase of +6 , +22, and +45% for Cd, Zn, and Mo concentrations, respectively from core A to C is primarily driven by TOC loss (up to ca. ˜21%) during catagenesis, as demonstrated by Dickson et al. (2020) through pyrolysis experiments on the same core material.

The magnitude of change in Hg content compared to previously determined TOC loss (Dickson et al. 2020) shows that less than half the increase in Hg can be explained by mass loss during catagenesis. This implies that, in addition to the constant sum effects discussed above, other processes likely have played role. Such processes could include, for example, internal redistribution of Hg in the sediment or capture of extraneous Hg within the Posidonienschiefer. Hg mobility during maturation might, for example, be attributed to volatility of weakly bound Hg^0 and Hg^{2+} at relatively low temperatures (60 to 225 °C) (Rumayor et al., 2013), which overlaps with catagenesis temperature experienced by this sequence in the Lower Saxony Basin (50 to 330 °C) (Bruns et al., 2013). In addition to the rise in average Hg content, its value is rather stable in core A, whereas an up-section increase is observed in cores B and C (Fig. 6). While this might be suggestive of Hg migration and (partial) recapture, this is difficult to envisage in lithologies such as the Posidonienschiefer that have extremely low matrix porosity and permeability, especially after burial to depths in excess of 8 km (Hooker et al., 2020).

An alternative explanation might be that the TOC, TS and Hg of core B and C were slightly higher in the upper interval at the time of deposition. Although the basin is generally characterised by euxinic conditions, the presumed greater palaeo-water depths of core B and C and thereby relative thicknesses of the euxinic water column may have resulted in slightly higher TOC, TS and Hg at the time of deposition.

From the correlation between Hg, TOC, and TS in Table 2., Hg correlates significantly with TOC and TS in all cores, without there being correlation between TOC and TS. The relationship indicates the tendency of Hg likely being hosted in both the organic C fraction and sulfur compounds which add complexity to the mechanism of redistribution/re-capture of Hg during thermal maturation.

5.3. Potential mechanisms of perceived Hg enrichment: fractures, and fluid (hydrocarbon) migration or different starting conditions?

The maturation of organic matter and heating of sediments ultimately can lead to fluid overpressures and fracturing of low-porosity/permeability rocks. For example, according to Meissner (1978), the catagenesis of solid kerogen into liquid hydrocarbons, gas, residue and other by-products is accompanied by a volume expansion of up to 25%. It has been suggested that this volume-change reaction would increase local fluid pressures resulting in hydraulic fracturing and formations of veins (e.g., Mandl & Harkness, 1987; Lash & Engelder, 2005). Shale layers in cores B and C contain abundant layer-parallel and oblique veins, mostly filled by calcite cement, with traces of pyrite crystals (Hooker et al., 2020). These oblique and bedding-parallel fractures containing so-called 'beef' calcite may have played an important role in the primary migration of petroleum fluids within and from the Posidonienschiefer (Leythaeuser et al., 1988), but, as Hooker et al. (2020) indicate, the potential for vertical migration through the fractures that are filled with calcite is low,

as well as the postulated porosity and permeability within the fracture fill. Whether large-scale fractures or networks of fractures existed outside the cored interval and facilitated fluid migration cannot be established with the present material.

Alternatively, core B and C may have had slightly higher Hg during deposition, due to their higher TOC content. However, if we assume that Hg/TOC of the immature core (˜11 ppb/%) is representative of the original Hg/TOC of cores B and C and that Hg in these cores did not change, the TOC loss in those cores would need to be ˜45% to reach the observed Hg content. A loss of 45% far exceeds the observed TOC loss during pyrolysis experiments (21%, Dickson et al. 2020) and is inconsistent with enrichments other trace element data. This implies that, if starting conditions were different, Hg/TOC for cores B and C should have been substantially higher than for core A. Such higher Hg/TOC and Hg/TS seems unlikely given their distal position in the basin and greater potential for strongly reducing conditions, which typically lead to reduced, not increased, Hg/TOC and Hg/TS (Them et al., 2019; Grasby et al., 2019; Shen et al., 2022; Frieling et al., in review).

5.4. Implications for the use of the Hg proxy in mature sediments

For the compiled data of Grasby et al. (2019) that includes both background and events with active LIPs, average shale values of 62.4 ppb and 71.9 ppb/%TOC are given. The "peak" of Hg contents (397 ppb and 433 ppb) in mature cores B and C (Fig. 3 and 4) are in the range of "Hg spikes" in the geological record previously interpreted to result from LIP activity (e.g., ˜20 ppb Hg, associated with the Early Cretaceous Greater Ontong Java LIP (Charbonnier & Föllmi, 2017) to 2517 ppb Hg at the Frasnian–Famennian (Devonian) transition (Racki et al., 2018)). However, the TOC-normalised Hg in the two mature cores (56 ppb/% and 48 ppb/ %) are not in the range of recorded Hg/TOC generally considered as volcanic peaks (e.g., ˜175 ppb/ % at the Greater Ontong Java LIP and 7102 ppb/ % at the Frasnian-Famennian transition). The Hg peaks in cores B and C (397-433 ppb) likely resulted from Hg redistribution and rock mass loss during thermal maturation, yet the maximum Hg content is similar to the peak Hg anomaly in Siberian Traps (396 ppb) (Wang et al., 2018) and Deccan Traps (415 ppb) (Sial et al., 2013).

The divergence of the Hg/TOC and Hg/TS above 50 m relative depth (Fig. 6) in cores B and C from a stable signal of Hg/TOC and Hg/TS in core A is difficult to explain without a degree of Hg redistribution and/or slightly higher Hg for the upper Posidonienschiefer in core B and C (see section 5.3). Regardless of the mechanism, the increase in Hg/TOC from TOC alone implies knowledge of thermal maturation history of the material becomes critical for the interpretation of Hg records when analysing sediments that have been exposed to significant temperatures. For example, if the elevated Hg/TOC in core B and C were to be interpreted without the context of core A and associated thermal maturity data, it might be interpreted as increased Hg loading or variability at the time of deposition. It is obvious from our findings that data from successions with significant calcite veins from hydrocarbon migration or other high-temperature fluid migration, similar to those observed in the Posidonienschiefer should be treated with extreme caution. Lastly, we cannot exclude that veins formed during, for example, (non-thermal) fluid escape could have served as similar pathways for Hg redistribution.

Thermally mature sediments have been previously used to assess the potential role of volcanic Hg enrichment in the T-OAE (e.g., East Tributary and core 1-35-62-5W6 (Canada) with Tmax > 450 °C shows peak Hg/TOC of 58 ppb/% and 28 ppb/% respectively (Them et al., 2019), which is in the range of Hg/TOC found in cores B and C). However, if in fact the mercury content increased simultaneously with the loss of TOC during thermal maturation, as suggested by our results here, it could imply that the Hg and Hg/TOC in these more mature and overmature Canadian cores might overestimate Hg loading compared to immature sections elsewhere. When comparing the Canadian T-OAE core material to other T-OAE sections (e.g., Bornholm, Denmark section with Hg/TOC 2590 ppb/% (Percival et al., 2015) and El Peñon, Chile with Hg/TOC 234 ppb/% (Fantasia et al., 2018)), there is no tell-tale sign they are systemically biased. This is likely because the increase in (normalised) Hg introduced by thermal maturation is small relative to the local and (supra)regional variability in Hg deposition (Lepland et al., 2010; Leipe et al., 2013; Percival et al., 2018; Them et al., 2019) and would likely go unnoticed unless the effects of burial-related heating can be

isolated, as we have done here. For periods when all records are thermally mature as would be progressively more likely with sediment deposited further back in time, systematic increases in Hg and normalised Hg with thermal maturity could lead to overestimated volcanic (Hg) emissions.

6. Conclusions

We studied three cores spanning the same formation with different levels of thermal maturity from the Lower Toarcian Posidonienschiefer in the Lower Saxony Basin, Germany. We show the increases of Hg content in mature core B and overmature core C were as high as +132% to +157% relative to the immature core A. Because thermal maturation also reduced the TOC content of the host rock at high levels of maturity, Hg/TOC ratios from mature sediments are considerably inflated. Consequently, the use of Hg and Hg/TOC ratios in mature organic-rich shale could lead to overestimates of Hg inventories in the geological past. Further, the magnitude of Hg enrichment is much larger than observed for other trace metals (e.g., Mo, Cd, Zn), which implies that the loss of mass caused by expulsion of hydrocarbons as a result of thermal maturation might not be the only process involved in causing elevated Hg content.

Mature cores B and C showed high Hg content variability profile in contrasts with the relatively stable Hg content profile in core A. We argue that the pronounced difference in the stratigraphic signals might be explained by the mobility and volatility of Hg in the temperature range of thermal maturation in the LSB, the precise mechanisms of mobilisation and re-sequestration remain elusive. Specifically, the observed fractures in cores B and C may have allowed Hg to migrate and re-adsorb at key levels in the stratigraphy, although there is still large uncertainty how this would effectively permeate the bulk of the lithology due to the extremely low matrix porosity and permeability of the Posidonienschiefer.

In general, the magnitude of elevated Hg content and TOC-normalised Hg in the mature cores (B and C) found here is not as high as Hg peak values interpreted as mercury perturbations caused by LIP volcanism. Nonetheless, our results show that the thermal history of sediments must be considered when using Hg as a proxy for volcanism. Specifically, the >2-fold enrichment in Hg content associated with maturation and the potential influence of fluid migration leading to levels of relative Hg enrichment warrant a cautious approach when using (over)mature and especially fractured sedimentary successions as an archive for far-field subaerial volcanic activity.

Hg mobilization processes during thermal maturation, hydrocarbon expulsion and migration history should be considered in evaluating Hg in oil and gas reservoirs. It is essential not only to think about Hg content in the original immature source rock but also how sediment thermal maturity level might enrich or, oppositely, reduce Hg content in the final product

Acknowledgments

We thank S. Wyatt (University of Oxford) and J. Brakeley (Royal Holloway University of London) for analytical assistance. Funding was provided from European Research Council Consolidator Grant (ERC-2018-COG-818717-V-ECHO). Special thanks to Shell Global Solutions B.V. for access to samples for this study. A.I. is supported by a Jardine Foundation scholarship.

Data Availability Statement

All newly generated data will be made available through a permanent online data repository upon publication.

References

Abarghani, A., Gentzis, T., Liu, B., Khatibi, S., Bubach, B., & Ostadhassan, M. (2020). Preliminary investigation of the effects of thermal maturity on redox-sensitive trace metal concentration in the Bakken source rock, North Dakota,. *American Chemical Society Omega* , *5* (13), 7135–7148. https://doi.org/10.1021/acsomega.9b03467

Behar, F., Beaumont, V., & De B. Penteado, H. L. (2001). Rock-Eval 6 technology: performances and developments. *Oil & Gas Science and Technology* , *56* (2), 111–134. https://doi.org/10.2516/ogst:2001013

Benoit, J. M., Mason, R. P., Gilmour, C. C., & Aiken, G. R. (2001). Constants for mercury binding by organic matter isolates from the Florida Everglades. *Geochimica et Cosmochimica Acta* ,*65* (24), 4445–4451. https://doi.org/10.1016/S0016-7037(01)00742-6

Betz, D., Führer, F., Greiner, G., & Plein, E. (1987). Evolution of the Lower Saxony Basin. *Tectonophysics* , *137* (1–4). https://doi.org/10.1016/0040-1951(87)90319-2

Bin, C., Xiaoru, W., & Lee, F. S. C. (2001). Pyrolysis coupled with atomic absorption spectrometry for the determination of mercury in Chinese medicinal materials. *Analytica Chimica Acta* ,*447* (1–2), 161–169. https://doi.org/10.1016/S0003-2670(01)01218-1

Blumenberg, M., Zink, K. G., Scheeder, G., Ostertag-Henning, C., & Erbacher, J. (2019). Biomarker paleo-reconstruction of the German Wealden (Berriasian, Early Cretaceous) in the Lower Saxony Basin (LSB).*International Journal of Earth Sciences, 108,* 229–244. https://doi.org/10.1007/s00531-018-1651-5

Brink, H. J., Durschner, H., & Trappe, H. (1992). Some aspects of the late and post-Variscan development of the Northwestern German Basin.*Tectonophysics* , *207* (1–2), 65–95. https://doi.org/10.1016/0040-1951(92)90472-I

Bruns, B., di Primio, R., Berner, U., & Littke, R. (2013). Petroleum system evolution in the inverted Lower Saxony Basin, northwest Germany: A 3D basin modeling study. *Geofluids* , *13* (2), 246–271. https://doi.org/10.1111/gfl.12016

Carvajal-Ortiz, H., Gentzis, T., & Ostadhassan, M. (2021). Sulfur differentiation in organic-rich shales and carbonates via open-system programmed pyrolysis and oxidation: insights into fluid souring and H_2S production in the Bakken Shale, United States.*Energy and Fuels* , *35* (15), 12030–12044. https://doi.org/10.1021/acs.energyfuels.1c01562

Chappaz, A., Lyons, T. W., Gregory, D. D., Reinhard, C. T., Gill, B. C., Li, C., & Large, R. R. (2014). Does pyrite act as an important host for molybdenum in modern and ancient euxinic sediments? *Geochimica et Cosmochimica Acta* , *126* , 112–122. https://doi.org/10.1016/j.gca.2013.10.028

Charbonnier, G., & Follmi, K. B. (2017). Mercury enrichments in lower Aptian sediments support the link between Ontong Java large igneous province activity and oceanic anoxic episode 1a. *Geology* ,*45* (1), 63–66. https://doi.org/10.1130/G38207.1

Dahl, T. W., Chappaz, A., Hoek, J., McKenzie, C. J., Svane, S., & Canfield, D. E. (2017). Evidence of molybdenum association with particulate organic matter under sulfidic conditions. *Geobiology* ,*15* (2), 311–323. https://doi.org/10.1111/gbi.12220

Dickson, A. J., Idiz, E., Porcelli, D., & van den Boorn, S. H. J. M. (2020). The influence of thermal maturity on the stable isotope compositions and concentrations of molybdenum, zinc and cadmium in organic-rich marine mudrocks. *Geochimica et Cosmochimica Acta* ,*287* , 205–220. https://doi.org/10.1016/j.gca.2019.11.001

Dickson, A. J., Idiz, E., Porcelli, D., Murphy, M. J., Celestino, R., Jenkyns, H. C., et al. (2022). No effect of thermal maturity on the Mo, U, Cd, and Zn isotope compositions of Lower Jurassic organic-rich sediments. *Geology* , *50* (5), 598–602. https://doi.org/10.1130/g49724.1

Fadeeva, V. P., Tikhova, V. D., & Nikulicheva, O. N. (2008). Elemental analysis of organic compounds with the use of automated CHNS analyzers.*Journal of Analytical Chemistry* , *63* (11), 1094–1106. https://doi.org/10.1134/S1061934808110142

Fantasia, A., Follmi, K. B., Adatte, T., Bernardez, E., Spangenberg, J. E., & Mattioli, E. (2018). The Toarcian oceanic anoxic event in southwestern Gondwana: An example from the Andean Basin, northern Chile.*Journal of the Geological Society* , *175* (6), 883–902. https://doi.org/10.1144/jgs2018-008

French, K.L., Sepulveda, J., Trabucho-Alexandre, J., Grocke, D.R., & Summons, R.E. (2014). Organic geochemistry of the early Toarcian oceanic anoxic event in Hawsker Bottoms, Yorkshire, England. *Earth and Planetary Science Letters* , *390* , 116-127. https://doi.org/10.1016/j.epsl.2013.12.033

Frieling J., Mather T. A., Marz C., Jenkyns H. C., Hennekam R., Reichart G., Slomp C. P., & van Helmond N. A. G. M. (2022). Effects of redox variability and early diagenesis on marine sedimentary Hg records. ESSOAr. Preprint. https://doi.org/10.1002/essoar.10512647.1

Celestino, R. (2019). Environmental change and carbon cycling during the Early Jurassic : A multi-proxy study on the Posidonienschiefer of NW Germany, (Doctoral dissertation). (http://hdl.handle.net/10871/36576). Exeter, UK. University of Exeter.

Fitzgerald, W. F., Lamborg, C. H., & Hammerschmidt, C. R. (2007). Marine biogeochemical cycling of mercury. *Chemical Reviews* ,*107* (2), 641–662. https://doi.org/10.1021/cr050353m

Frimmel, A., Oschmann, W., & Schwark, L. (2004). Chemostratigraphy of the Posidonia Black Shale, SW Germany I. Influence of sea-level variation on organic facies evolution. *Chemical Geology* ,*206* (3–4), 199–230. https://doi.org/10.1016/j.chemgeo.2003.12.007

Gajdosechova, Z., Boskamp, M. S., Lopez-Linares, F., Feldmann, J., & Krupp, E. M. (2016). Hg speciation in petroleum hydrocarbons with emphasis on the reactivity of Hg particles. *Energy and Fuels* ,*30* (1), 130–137. https://doi.org/10.1021/acs.energyfuels.5b02080

Gehrke, G. E., Blum, J. D., & Meyers, P. A. (2009). The geochemical behavior and isotopic composition of Hg in a mid-Pleistocene western Mediterranean sapropel. *Geochimica et Cosmochimica Acta* ,*73* (6), 1651–1665. https://doi.org/10.1016/j.gca.2008.12.012

Grasby, S. E., Shen, W., Yin, R., Gleason, J. D., Blum, J. D., Lepak, R. F., et al. (2017). Isotopic signatures of mercury contamination in latest Permian oceans. *Geology* , *45* (1), 55–58. https://doi.org/10.1130/G38487.1

Grasby, S. E., Them, T. R., Chen, Z., Yin, R., & Ardakani, O. H. (2019). Mercury as a proxy for volcanic emissions in the geologic record. *Earth-Science Reviews* , *196* (March), 102880. https://doi.org/10.1016/j.earscirev.2019.102880

Hooker, J. N., Ruhl, M., Dickson, A. J., Hansen, L. N., Idiz, E., Hesselbo, S. P., & Cartwright, J. (2020). Shale anisotropy and natural hydraulic fracture propagation: An example from the Jurassic (Toarcian) Posidonienschiefer, Germany. *Journal of Geophysical Research: Solid Earth* , *125* (3), 1–14. https://doi.org/10.1029/2019JB018442

Jenkyns, H. C. (1985). The Early Toarcian and Cenomanian-Turonian anoxic events in Europe: comparisons and contrasts. *Geologische Rundschau, 74* (3), 505-518. https://doi.org/10.1007/BF01821208

Jenkyns, H. C. (1988). The early Toarcian (Jurassic) anoxic event; stratigraphic, sedimentary and geochemical evidence. *American Journal of Science* , *288* (2), 101-151. https://doi.org/10.2475/ajs.288.2.101

Jones, M. T., Percival, L. M. E., Stokke, E. W., Frieling, J., Mather, T. A., Riber, L., et al. (2019). Mercury anomalies across the Palaeocene-Eocene Thermal Maximum. *Climate of the Past* ,*15* (1), 217–236. https://doi.org/10.5194/cp-15-217-2019

Krupp, R. (1988). Physicochemical aspects of mercury metallogenesis. *Chemical Geology* , *69* (3–4), 345–356. https://doi.org/10.1016/0009-2541(88)90045-9

Lamborg, C. H., Fitzgerald, W. F., Damman, A. W. H., Benoit, J. M., Balcom, P. H., & Engstrom, D. R. (2002a). Modern and historic atmospheric mercury fluxes in both hemispheres: Global and regional mercury cycling implications. *Global Biogeochemical Cycles* ,*16* (4), 1104. https://doi.org/10.1029/2001gb001847

Lamborg, C. H., Fitzgerald, W. F., O'Donnell, J., & Torgersen, T. (2002b). A non-steady-state compartmental model of global-scale mercury biogeochemistry with interhemispheric atmospheric gradients. *Geochimica*

et Cosmochimica Acta , *66* (7), 1105–1118. https://doi.org/10.1016/S0016-7037(01)00841-9

Lash, G. G., & Engelder, T. (2005). An analysis of horizontal microcracking during catagenesis: Example from the Catskill delta complex. *American Association of Petroleum Geologists Bulletin* ,*89* (11), 1433–1449. https://doi.org/10.1306/05250504141

Leipe, T., Moros, M., Kotilainen, A., Vallius, H., Kabel, K., Endler, M., & Kowalski, N. (2013). Mercury in Baltic Sea sediments - Natural background and anthropogenic impact. *Geochemistry* , *73* (3), 249–259. https://doi.org/10.1016/j.chemer.2013.06.005

Lepland, A., Andersen, T. J., Lepland, A., Arp, H. P. H., Alve, E., Breedveld, G. D., & Rindby, A. (2010). Sedimentation and chronology of heavy metal pollution in Oslo harbor, Norway. *Marine Pollution Bulletin* , *60* (9), 1512–1522. https://doi.org/10.1016/j.marpolbul.2010.04.017

Lewan, M. D., Winters, J. C., & Mcdonald, J. H. (1979). Generation of oil-like pyrolyzates from organic-rich shales. *Science, 203* (4383), 897–899. http://www.jstor.org/stable/1747886

Lewan, M. D., & Maynard, J. (1982). Factors controlling enrichment of vanadium and nickel in the bitumen of organic sedimentary rocks.*Geochimica et Cosmochimica Acta* , *46* (12), 2547–2560. https://doi.org/10.1016/0016-7037(82)90377-5

Leythaeuser, D., Littke, R., Radke, M., & Schaefer, R. G. (1988). Geochemical effects of petroleum migration and expulsion from Toarcian source rocks in the Hils syncline area, NW-Germany. *Organic Geochemistry* , *13* (1–3), 489–502. https://doi.org/10.1016/0146-6380(88)90070-8

Lindqvist, O., Johansson, K., Bringmark, L., Timm, B., Aastrup, M., Andersson, A., et al. (1991). Mercury in the Swedish environment - Recent research on causes, consequences and corrective methods. *Water, Air, & Soil Pollution* , *55* (1–2). https://doi.org/10.1007/BF00542429

Littke, R., Baker, D. R., & Leythaeuser, D. (1988). Microscopic and sedimentologic evidence for the generation and migration of hydrocarbons in Toarcian source rocks of different maturities. *Organic Geochemistry* , *13* (1–3), 549–559. https://doi.org/10.1016/0146-6380(88)90075-7

Littke, R., Leythaeuser, D., Rullkotter, J., & Baker, D. R. (1991). Keys to the depositional history of the Posidonia Shale (Toarcian) in the Hils Syncline, northern Germany. *Geological Society Special Publication* , *58* (58), 311–333. https://doi.org/10.1144/GSL.SP.1991.058.01.20

Liu Z., Tian H., Yin R., Chen D., & Gai H. (2022) Mercury loss and isotope fractionation during thermal maturation of organic-rich mudrocks. *Chemical Geology* , *612* , 121144. https://doi.org/10.1016/j.chemgeo.2022.121144

Mandl, G., & Harkness, R. M. (1987). Hydrocarbon migration by hydraulic fracturing. *Geological Society Special Publication* , *29* , 39–53. https://doi.org/10.1144/GSL.SP.1987.029.01.04

Mason, R. P., Fitzgerald, W. F., & Morel, F. M. M. (1994). The biogeochemical cycling of elemental mercury: Anthropogenic influences.*Geochimica et Cosmochimica Acta* , *58* (15), 3191–3198. https://doi.org/10.1016/0016-7037(94)90046-9

Meissner, F. F. (1978). Petroleum geology of the Bakken formation Williston basin, North Dakota and Montana. In D. Estelle, R. Miller (Eds.), *Montana Geological Society: 24th Annual Conference: 1978 Williston Basin Symposium* (pp. 207-227). Billings, MT: Montana Geological Society.

Mukherjee, A. B., Bhattacharya, P., Sarkar, A., & Zevenhoven, R. (2009). Mercury emissions from industrial sources in India and its effects in the environment. In R. Mason & N. Pirrone (Eds.),*Mercury fate and transport in the global atmosphere: Emissions, measurements and models* (pp. 81–112). Boston, MA: Springer US. https://doi.org/10.1007/978-0-387-93958-2_4

Outridge, P. M., Sanei, H., Stern, G. A., Hamilton, P. B., & Goodarzi, F. (2007). Evidence for control of

mercury accumulation rates in Canadian High Arctic Lake sediments by variations of aquatic primary productivity. *Environmental Science and Technology* ,*41* (15), 5259–5265. https://doi.org/10.1021/es070408x

Outridge, P. M., Stern, G. A., Hamilton, P. B., & Sanei, H. (2019). Algal scavenging of mercury in preindustrial Arctic lakes.*Limnology and Oceanography* , *64* (4), 1558–1571. https://doi.org/10.1002/lno.11135

Percival, L. M. E., Bergquist, B. A., Mather, T. A., & Sanei, H. (2021). Sedimentary mercury enrichments as a tracer of large igneous province volcanism. In R.E. Ernst, A.J. Dickson and A. Bekker (Eds.),*Large igneous provinces: A driver of global environmental and biotic changes, Geophysical Monograph Series* (Vol. 255, pp. 247–262). Washington, DC and Hoboken, NJ: American Geophysical Union and John Wiley and Sons, Inc. https://doi.org/10.1002/9781119507444.ch11

Percival, L. M. E., Witt, M. L. I., Mather, T. A., Hermoso, M., Jenkyns, H. C., Hesselbo, S. P., et al. (2015). Globally enhanced mercury deposition during the end-Pliensbachian extinction and Toarcian OAE : A link to the Karoo – Ferrar Large Igneous Province. *Earth and Planetary Science Letters* , *428* , 267–280. https://doi.org/http://dx.doi.org/10.1016/j.epsl.2015.06.064

Percival, L. M. E., Jenkyns, H. C., Mather, T. A., Dickson, A. J., Batenburg, S. J., Ruhl, M., et al. (2018). Does large igneous province volcanism always perturb the mercury cycle? Comparing the records of Oceanic Anoxic Event 2 and the end-Cretaceous to other Mesozoic events.*American Journal of Science* , *318* (8), 799–860. https://doi.org/10.2475/08.2018.01

Peters, K. E., & Cassa, M. R. (1994). Applied source rock geochemistry. In L.B. Magoon, W.G. Dow (Eds.), *The petroleum system—from source to trap* , *American Association of Petroleum Geologists Memoir* (Vol. 60, pp 93–120). Tulsa, OK: The American Association of Petroleum Geologists.

Pyle, D. M., & Mather, T. A. (2003). The importance of volcanic emissions for the global atmospheric mercury cycle. *Atmospheric Environment* , *37* (36), 5115–5124. https://doi.org/10.1016/j.atmosenv.2003.07.011

Racki, G., Rakocinski, M., Marynowski, L., & Wignall, P. B. (2018). Mercury enrichments and the Frasnian-Famennian biotic crisis: A volcanic trigger proved? *Geology* , *46* (6), 543–546. https://doi.org/10.1130/G40233.1

Raiswell, R., & Berner, R. A. (1987). Organic carbon losses during burial and thermal maturation of normal marine shales. *Geology* ,*15* (9), 853–856. https://doi.org/10.1130/0091-7613(1987)15<853:OCLDBA>2.0.CO;2

Riegraf, W., Werner, G., & Lorcher, F. (1984). Der Posidonienschiefer: Biostratigraphie, Fauna und Fazies des sudwestdeutschen Untertoarciums (Lias Epsilon). Stuttgart: F. Enke, 195pp.

Rohl, H. J., Schmid-Rohl, A., Oschmann, W., Frimmel, A., & Schwark, L. (2001). The Posidonia Shale (Lower Toarcian) of SW-Germany: An oxygen-depleted ecosystem controlled by sea level and palaeoclimate.*Palaeogeography, Palaeoclimatology, Palaeoecology* ,*165* (1–2), 27–52. https://doi.org/10.1016/S0031-0182(00)00152-8

Rullkotter, J., Leythaeuser, D., Horsfield, B., Littke, R., Mann, U., Muller, P. J., et al. (1988). Organic matter maturation under the influence of a deep intrusive heat source: A natural experiment for quantitation of hydrocarbon generation and expulsion from a petroleum source rock (Toarcian shale, northern Germany). *Organic Geochemistry* , *13* (4–6), 847–856. https://doi.org/10.1016/0146-6380(88)90237-9

Rullkotter, Jurgen, & Marzi, R. (1988). Natural and artificial maturation of biological markers in a Toarcian shale from northern Germany. *Organic Geochemistry* , *13* (4–6), 639–645. https://doi.org/10.1016/0146-6380(88)90084-8

Rumayor, M., Diaz-Somoano, M., Lopez-Anton, M. A., & Martinez-Tarazona, M. R. (2013). Mercury compounds characterization by thermal desorption. *Talanta* , *114* , 318–322. https://doi.org/10.1016/j.talanta.2013.05.059

Sanei, H. (2020). Genesis of solid bitumen. *Scientific Reports* ,*10* (1), 1–10. https://doi.org/10.1038/s41598-020-72692-2

Sanei, H., Grasby, S. E., & Beauchamp, B. (2012). Latest Permian mercury anomalies. *Geology* , *40* (1), 63–66. https://doi.org/10.1130/G32596.1

Scaife, J. D., Ruhl, M., Dickson, A. J., Mather, T. A., Jenkyns, H. C., Percival, L. M. E., et al. (2017). Sedimentary Mercury Enrichments as a Marker for Submarine Large Igneous Province Volcanism? Evidence From the Mid-Cenomanian Event and Oceanic Anoxic Event 2 (Late Cretaceous).*Geochemistry, Geophysics, Geosystems* , *18* (12), 4253–4275. https://doi.org/10.1002/2017GC007153

Schmid-Rohl, A., Rohl, H. J., Oschmann, W., Frimmel, A., & Schwark, L. (2002). Palaeoenvironmental reconstruction of Lower Toarcian epicontinental black shales (Posidonia Shale, SW Germany): Global versus regional control. *Geobios* , *35* (1), 13–20. https://doi.org/10.1016/S0016-6995(02)00005-0

Schwark, L., & Frimmel, A. (2004). Chemostratigraphy of the Posidonia Black Shale, SW-Germany II. Assessment of extent and persistence of photic-zone anoxia using aryl isoprenoid distributions. *Chemical Geology* , *206* (3–4), 231–248. https://doi.org/10.1016/j.chemgeo.2003.12.008

Shen, J., Feng, Q., Algeo, T. J., Liu, J., Zhou, C., Wei, W., et al. (2020). Sedimentary host phases of mercury (Hg) and implications for use of Hg as a volcanic proxy. *Earth and Planetary Science Letters* , *543* , 116333. https://doi.org/10.1016/j.epsl.2020.116333

Shen, J., Algeo, T.J., & Feng, Q. (2022). Mercury isotope evidence for a non-volcanic origin of Hg spikes at the Ordovician-Silurian boundary, South China. *Earth and Planetary Science Letters, 594* , 117705. https://doi.org/10.1016/j.epsl.2022.117705

Sial, A. N., Lacerda, L. D., Ferreira, V. P., Frei, R., Marquillas, R. A., Barbosa, J. A., et al. (2013). Mercury as a proxy for volcanic activity during extreme environmental turnover : The Cretaceous – Paleogene transition. *Palaeogeography, Palaeoclimatology, Palaeoecology* , *387* , 153–164. https://doi.org/10.1016/j.palaeo.2013.07.019

Song, J., Littke, R., & Weniger, P. (2017). Organic geochemistry of the Lower Toarcian Posidonia Shale in NW Europe. *Organic Geochemistry* , *106* , 76-92. https://doi.org/10.1016/j.orggeochem.2016.10.014

Them, T. R., Jagoe, C. H., Caruthers, A. H., Gill, B. C., Grasby, S. E., Grocke, D. R., et al. (2019). Terrestrial sources as the primary delivery mechanism of mercury to the oceans across the Toarcian Oceanic Anoxic Event (Early Jurassic). *Earth and Planetary Science Letters* , *507* , 62–72. https://doi.org/10.1016/j.epsl.2018.11.029

Tissot, B. P., & Welte, D. H. (1984). Sedimentary processes and the accumulation of organic matter. In Tissot, B.P., Welte, D.H.,*Petroleum Formation and Occurrence* (pp. 55–62). Berlin: Springer-Verlag. https://doi.org/10.1007/978-3-642-96446-6_5

UN Environment. (2019). *Global Mercury Assessment 2018* . UN Environment Programme, Chemicals and Health Branch Geneva, Switzerland.

Wallace, G. T. (1982). The association of copper, mercury and lead with surface-active organic matter in coastal seawater. *Marine Chemistry* , *11* (4), 379–394. article. https://doi.org/10.1016/0304-4203(82)90032-9

Wang, X., Cawood, P. A., Zhao, H., Zhao, L., Grasby, S. E., Chen, Z. Q., et al. (2018). Mercury anomalies across the end Permian mass extinction in South China from shallow and deep water depositional environments.*Earth and Planetary Science Letters* , *496* , 159–167. https://doi.org/10.1016/j.epsl.2018.05.044

Wang, Z., Tan, J., Boyle, R., Wang, W., Kang, X., Dick, J., & Lyu, Q. (2020). Mercury anomalies within the lower Cambrian (stage 2–3) in South China: Links between volcanic events and paleoecology.*Palaeogeography, Palaeoclimatology, Palaeoecology* ,*558* (April). https://doi.org/10.1016/j.palaeo.2020.109956

Wilhelm, M., & Bloom, N. (2000). Mercury in petroleum. *Fuel Processing Technology* , *63* (1), 1–27. https://doi.org/10.1016/S0378-3820(99)00068-5

Wilhelm, S. M. (2001). Estimate of mercury emissions to the atmosphere from petroleum. *Environmental Science and Technology* ,*35* (24), 4704–4710. https://doi.org/10.1021/es001804h

Wilkes, H., Disko, U., & Horsfield, B. (1998). Aromatic aldehydes and ketones in the Posidonia Shale, Hils Syncline, Germany. *Organic Geochemistry* , *29* (1–3), 107–117. https://doi.org/10.1016/S0146-6380(98)00138-7

Zaferani, S., Perez-rodriguez, M., & Biester, H. (2018). Diatom ooze—A large marine mercury sink. *Science, 361* (6404), 797-800. https://doi.org/10.1016/j.scitotenv.2020.143940

The influence of sediment thermal maturity and hydrocarbon formation on Hg behaviour in the stratigraphic record

A. O. Indraswari[1,2], J. Frieling[1], T. A. Mather[1], A. J. Dickson[3], H. C. Jenkyns[1], E. Idiz[1]

[1]Department of Earth Sciences, University of Oxford, South Parks Road, Oxford, OX1 3AN, UK.

[2]Geoscience Study Program, Faculty of Mathematics and Natural Sciences (FMIPA), Universitas Indonesia, Depok 16424, Indonesia.

[3]Centre of Climate, Ocean and Atmosphere, Department of Earth Sciences, Royal Holloway University of London, Egham, Surrey, TW20 0EX, UK.

Corresponding author: Asri O. Indraswari (asri.indraswari@exeter.ox.ac.uk)

Key Points:

- Thermal maturation of organic-rich deposits has increased Hg content > 2-fold
- Hg/TOC ratios from mature sediments are inflated because of organic carbon loss from the host rock during maturation
- Thermal history of sediments must be considered when using Hg as a proxy for volcanism

Abstract

While Hg in sediments is increasingly used as a proxy for deep-time volcanic activity, the behaviour of Hg in OM-rich sediments as they undergo thermal maturation is not well understood. In this study, we evaluate the effects of thermal maturation on sedimentary Hg contents and, thereby, the impact of thermal maturity on the use of the Hg/TOC proxy for large igneous province (LIP) volcanism. We investigate three cores (marine organic matter) with different levels of thermal maturity in lowermost Toarcian sediments (Posidonienschiefer) from the Lower Saxony Basin in Germany. We present Hg content, bulk organic geochemistry, and total sulfur in three cores with different levels of thermal maturity. The comparison of Hg data between the three cores indicates that Hg content in the mature/overmature sediments have increased > 2-fold compared to Hg in the immature deposits. Although difficult to confirm with the present data, we speculate that redistribution within the sedimentary sequence caused by the mobility and volatility of the element under relatively high temperatures may have contributed to Hg enrichment in distinct stratigraphic levels of the mature cores. Regardless of the exact mechanism, elevated Hg content together with organic-carbon loss by thermal maturation exaggerate the value of Hg/TOC in mature sediments, suggesting that thermal effects have to be considered when using TOC-normalised Hg as a proxy for far-field volcanic activity.

1. Introduction

Mercury (Hg) is highly toxic, which means that understanding its behaviour in shallow- and deep-earth environments and how it cycles through ecosystems is of considerable importance. Emissions of Hg into the atmosphere include those from natural sources, such as volcanic exhalations, and anthropogenic sources, such as artisanal and small-scale mining, fossil-fuel combustion, non-ferrous metal smelting, and cement production (UN Environment, 2019). Critically, a substantial part of these emissions is in gaseous form, and the relatively long atmospheric lifetime of Hg (0.5–2 years) means that it can be globally dispersed before deposition (e.g., Lindqvist et al., 1991; Mason et al., 1994; Lamborg et al., 2002a,b). It is generally assumed that most of the Hg will be finally sequestered in sediments containing organic matter (OM) as OM-Hg complexes. Indeed, field-data show that OM is usually the dominant Hg carrier, both in the water column and sediment (Wallace, 1982; Benoit et al., 2001; Outridge et al., 2007). In addition to OM, sulfides (e.g., HgS and Hg-inclusions in pyrite) and clays may prove significant sedimentary Hg hosts (Percival et al., 2018; Shen et al., 2020; Wang et al., 2020).

The behaviour of Hg once deposited into sedimentary archives is of interest for several reasons. The presence and levels of Hg in oils and their organic-rich petroleum source rocks is important as it is considered a contaminant in hydrocarbon fields. Mercury is found in hydrocarbons in highly varying concentrations (Wilhelm & Bloom, 2000). For example, fuel oils contain Hg with values ranging from 7 to 30,000 ppb, with a typical value being 3500 ppb (Wilhelm, 2001; Mukherjee et al., 2009). Knowledge about the presence and level of Hg in these hydrocarbon streams is essential because it can determine, amongst other things, decisions regarding processing facility design (e.g., the inclusion of costly removal units) to mitigate Hg pollution (Wilhelm & Bloom, 2000; Gajdosechova et al., 2016). The observed variable and potentially very high Hg content in hydrocarbons implies that it is critical to understand which sedimentary strata are likely to be enriched in Hg during deposition, and what processes might move and concentrate Hg into expelled fluids during thermal maturation of sediments.

Further to concerns regarding Hg behaviour in hydrocarbons, there has been much recent interest in the potential of Hg as a proxy for large-scale volcanism (namely large igneous provinces (LIP)) in the sedimentary record since volcanoes are amongst the largest natural sources (Pyle & Mather, 2003; Sanei et al., 2012; Percival et al., 2015; Scaife et al., 2017; Percival et al., 2021). Hg records are usually normalised to Total Organic Carbon (TOC) to correct for increases in Hg content associated with greater TOC contents (Sanei et al., 2012; Grasby et al., 2019). However, Hg can also be bound to sulfides and clay minerals and, in some environments, Hg deposition with such geochemical species may confound the usual sedimentary Hg-OM relationship (see e.g., Sanei et al., 2012; Charbonnier & Föllmi, 2017; Percival et al., 2018). Thus, several works (e.g., Grasby et al. (2019) and Shen et al. (2020)) have argued that it is critical to look at the relationship of Hg with TOC, as well as Hg variance with clay (Al) and total sulfur levels. Moreover, several previous studies acknowledge the

potential of changes to geological deep-time sedimentary Hg records induced by OM sources or types that, for example, may be related to coastal proximity (i.e., marine- *vs* terrestrial-derived OM; Grasby et al., 2017; Wang et al., 2018; Them et al., 2019). Various fixation mechanisms for Hg in organic-rich mudrocks have been investigated, including adsorption onto OM and clay minerals and incorporation of Hg into the crystal structures of other host minerals, particularly sulfides (Krupp, 1988; Shen et al., 2020). Pyrite-hosted Hg might become a more dominant phase when sediments are deposited under sulfidic conditions, where free H_2S occurs in the water column or sediment pore waters (Shen et al. 2020). However, whether these factors also lead to enhanced Hg sequestration or how these conditions affect proportioning between sedimentary host phases is not well constrained. While various potential confounding factors on sedimentary Hg distributions have been investigated (Grasby et al., 2019; Shen et al., 2020), the effects of thermal maturity on Hg content in deep-time sediments have not been tested systemically. This is however a critical knowledge gap as sedimentary Hg can be mobilised at temperatures known to be relevant for post-depositional sediment alteration and resulting oil and gas generation (e.g., Rumayor et al., 2013; Liu et al., 2022) and is clearly enriched in some hydrocarbon sources (e.g., Wilhelm, 2001; Mukherjee et al., 2009).

Thermal maturation of labile sedimentary OM occurs due to increasing temperature with increasing burial depth, typically on the order of ~30°C rise in temperature per kilometre of overburden. in catagenesis, that is conversion of kerogen, stable at lower temperatures, through thermal cracking into lower molecular weight components, loosely defined as bitumen. In the early stage of maturation, this bitumen contains a large proportion of high-molecular-weight compounds such as resins and asphaltenes. With increasing maturation, bitumen undergoes further cracking and disproportionation, resulting in lower molecular-weight hydrocarbon molecules and an insoluble coke-like C-rich residue: pyrobitumen (Tissot & Welte, 1984; Sanei, 2020). As the kerogen becomes more thermally 'mature' it progresses through the stages of oil and gas generation and, depending on the type of kerogen, potentially loses up to 60% of its organic matter mass due to migration of the generated products away from the host rock (Lewan et al., 1979; Tissot & Welte, 1984; Raiswell & Berner, 1987).

Thermal maturation may play a key role in altering the geochemical signature of metals (e.g., Mo, V, and Ni) due to the close association of these geochemical species with sedimentary OM and the transformations that OM undergoes (Lewan & Maynard, 1982; Chappaz et al., 2014; Dahl et al., 2017). For example, thermal maturation has been shown to lead to progressive enrichment in both the concentration of metals and their TOC-normalised values in sedimentary rocks for Mo, Zn, U and Cd (Dickson et al., 2020, 2022). Such increases can be attributed to the loss of mass caused by the removal of bitumen during thermal maturation and the minor partitioning of metals into mobilized organic fluid phases (Dickson et al., 2020, 2022). The generation of H_2O, CO_2, and H_2S from both the organic and inorganic phases in the rocks also might play a role in causing additional mass losses (Abarghani et al., 2020; Dickson et al., 2020).

However, it is difficult to directly measure metals bound to kerogen since the primary method to isolate this organic component is by digesting the mineral matrix using strong acids such as HF and HCl, which can also leach metals from the kerogen itself. Therefore, the mechanistic behaviour of metals, including Hg, in OM-rich sediments as they undergo thermal maturation is still not well understood.

Unlike most metals, there is evidence from analytical methods that utilise thermal desorption that sediments exposed to temperatures during burial typical of sedimentary basins (60–225 °C) could mobilise some Hg compounds (e.g., elemental Hg, weakly absorbed Hg, Hg-halides) (Rumayor et al., 2013, Liu et al. 2022), but the combined effects of prolonged exposure to the pressure and temperature regimes that typically exist during maturation remain untested.

Our study explores the influence of thermal maturation on sedimentary Hg using three cores covering a wide range of thermal maturity from the Lower Saxony Basin, Germany. By investigating Hg, bulk OM characteristics and total sulfur contents in a stratigraphically constrained interval from a single basin, we examined the role of thermal maturation as a key factor in post-depositional Hg mobility in sediments. We focus on the part of the Posidonienschiefer that stratigraphically sits above the negative carbon-isotope excursion characteristic of the Toarcian Oceanic Anoxic Event (T-OAE).

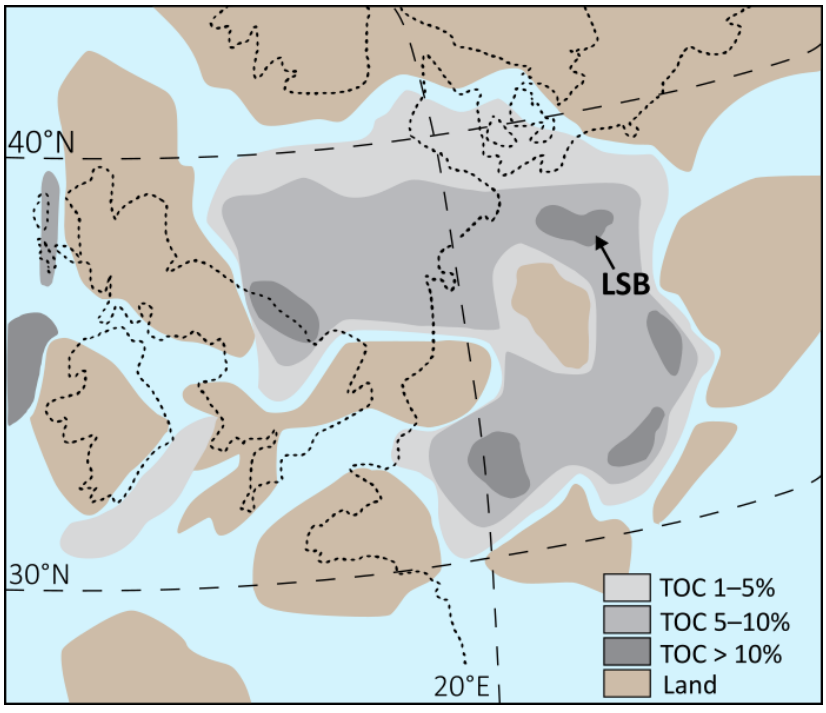

Figure 1. Location of the Lower Saxony Basin (LSB) in the Early Jurassic (ca.

182 Ma). Modern shorelines are shown as dashed lines. TOC—total organic carbon.

1. Geological Setting

The Lower Saxony Basin (LSB), located in north-western Germany (Fig. 1), is the country's most important oil province (Betz et al., 1987). It is a 300-km long and 65-km wide E–W-oriented basin formed during the breakup of the supercontinent Pangaea through extension and subsidence (Betz et al., 1987; Brink et al., 1992; Bruns et al., 2013). The Lower Toarcian Posidonienschiefer is a distinct organic-rich unit preserved in the LSB. For more than a century, this unit has been of scientific interest due to its importance as a source rock, including sedimentology (Littke et al., 1991; Röhl et al., 2001; Schmid-Röhl et al., 2002), stratigraphy (Riegraf et al., 1984; Frimmel et al., 2004; Schwark & Frimmel, 2004), petrology and geochemistry (Jenkyns, 1985, 1988; Leythaeuser et al., 1988; Rullkötter et al., 1988; Rullkötter & Marzi, 1988; Littke et al., 1988, 1991; Wilkes et al., 1998).

Evidence of persistent euxinia in the water column, and specifically indicators of free H_2S in the photic zone, comes from the identification of aryl isoprenoids and other carotenoids (isorenieratene) reported in the Posidonienschiefer from the LSB (Blumenberg et al., 2019) and from the Posidonia shales from other NW European basins (Schwark & Frimmel, 2004; French et al., 2014; Song et al., 2017). Redox conditions are important to consider when interpreting the variability of Hg records, which may result in enhanced Hg or subdued Hg sequestration and/or changes in sedimentary host-phase (e.g., Grasby et al., 2016; Them et al., 2019, Shen et al., 2019; Grasby et al., 2019; Frieling et al., 2022 PREPRINT). However, since the Posidonienschiefer was likely deposited under basin-wide euxinic conditions (Blumenberg et al., 2019), we do not expect differences in the Hg sequestration pathway between the analysed core localities. Because of high marine productivity and relatively minor influences of terrestrial OM (Rullkötter et al., 1988; Littke et al., 1991), major differences in OM-type between cores are also unlikely, excluding influences of variable proportions of marine and terrestrial OM on Hg loading.

Since its deposition in the Early Jurassic the Posidonienschiefer has been buried to various depths within the LSB, due to the effect of locally variable fault-bounded basin subsidence, followed by basin inversion during the Paleogene (Betz et al., 1987). As a result, the thermal maturity of the OM contained within the Posidonienschiefer varies over relatively short horizontal distances of tens of kilometres, making it a good candidate for testing whether thermal maturation can change the concentration of metals in organic-rich sedimentary rocks (Dickson et al., 2022).

Three ~30-m-long drilled cores containing stratigraphically equivalent sections of the Posidonienschiefer were retrieved from different parts of the LSB. Two of the cores (core A and B) have been studied previously to explore the maturation-dependent changes in stable-isotope compositions and concentrations of Mo, Zn,

Cd and U (Dickson et al., 2020, 2022) and the growth of the bed-parallel and oblique calcite veins known as 'beef' (Hooker et al., 2020). The thermal maturity of each core was established by reflectance measurements (%Ro) on terrestrial organic macerals (vitrinite~0.5% for core A (immature) and ~1.5% and ~3.5% (post-mature) for core B and core C, respectively. Because cores B and C lack a biostratigraphic framework, a core-to-core correlation is achieved via distinct basin-wide chemostratigraphic trends in the TOC and trace-metal records. Using the $^{13}C_{org}$ data for core A and subsequent correlation using the TOC of all three cores, we identify the interval of the Posidienschiefer that was deposited after the T-OAE, to avoid the Hg-cycle perturbation that characterises the T-OAE (Percival et al., 2015; Fantasia et al., 2018; Them et al., 2019).

3. Methods

A total of 647 samples (478 for core A, 121 for core B, and 48 for core C, with a stratigraphic resolution of 10 to 30 cm) were powdered and analysed for Hg content. Mercury content was measured on a Lumex RA-915 Portable Mercury Analyser coupled to a PYRO-915 pyrolysis unit at the University of Oxford (Bin et al., 2001). Powdered samples of between 50 and 100 mg were introduced into a sample boat, heated to >700 °C and left for up to 120 seconds to fully volatilize the Hg present. The instrument was calibrated before each run using NIST-SRM2587 (National Institute of Standards and Technology – Standard Reference Material: Trace Elements in Soil Containing Lead from Paint), with a Hg content of 290 ppb. The same standard was run for every ten samples to correct instrument drift. We calculate an external reproducibility of ±8.7% based on the repeat standard measurements (1 standard deviation (S.D.), n=199).

Hydrogen and oxygen indices (HI, OI) and TOC content data of all three cores have been published previously in Hooker et al. (2020). An additional 39 new samples (15 for core A, 21 for core B, and 3 for core C) were analysed with a Rock-Eval 6, following the methods in Behar et al. (2001), at the University of Oxford. The in-house standard SAB134 (Blue Lias organic-rich marl, 2.74 % TOC) was measured every 8 to 10 samples. The standard deviation of the in-house standard (SAB134) was ~0.03 % TOC (1 S.D.).

Analyses of total sedimentary sulfur (%TS) were undertaken on 155 samples (57 for core A, 50 for core B, and 48 for core C). An aliquot of each sample was wrapped in a tin capsule and then combusted using an Elemental Cube Elemental Analyzer Vario El III at the Department of Earth Sciences, Royal Holloway University of London (Carvajal-Ortiz et al., 2021; Fadeeva et al., 2008). A sulfanilamide reference standard (18.62 % S) was analysed at the start and end of each run and between every ten samples to monitor instrument drift. Within-run reproducibility calculated from the Eocene shale standards (1.24 % S) run as unknowns was ±0.12 % S (1 S.D., n=12).

High-resolution $^{13}C_{org}$ data from core A was measured by Celestino (2019). $^{13}C_{org}$ for core B and core C were analysed at the Open University (U.K). The

samples powders were prepared by decarbonating bulk sediments in 1M HCl before rinsing with de-ionised water until a neutral pH was reached. Samples were dried and re-powdered before being weighed into tin capsules and analysed using a Thermo MAT253 mass spectrometer coupled to a Flash HT combustion system. $^{13}C_{org}$ is expressed relative to the Vienna Pee Dee Belemnite (VPDB) scale via within-run calibration using NIST 8572 glutamic acid (-26.39 ‰), International Atomic Energy Agency (IAEA) CH-6 sucrose (-10.45 ‰) and L-Alanine (-23.33 ‰). Analytical precision, calculated from the 1 S.D. of L-alanine, is better than ±0.1 ‰.

4. Results

We focus on an interval of Posidonienschiefer that is stratigraphically above the negative carbon-isotope excursion characteristic of T-OAE (hereafter referred to as Posidonienschiefer). The stratigraphic successions of the cores in this study were tied together based on distinctive patterns in total organic carbon (TOC) following Dickson et al. (2022). The average TOC values of the Posidonienschiefer show an increase from core A to core B and from core B to core C (Table 1). Rock-Eval determined Hydrogen Index (HI) values in the section in core A average 687 mg hydrocarbons /g TOC (Fig. 2). By contrast, in cores B and C, the HI values throughout the Posidonienschiefer are relatively constant at near 0 (Fig. 3 and 4). Total sulfur (TS) content is ranging from 1.5 to 6 % for cores A, B, and C through the Posidonienschiefer, (Fig. 2, 3, and 4).

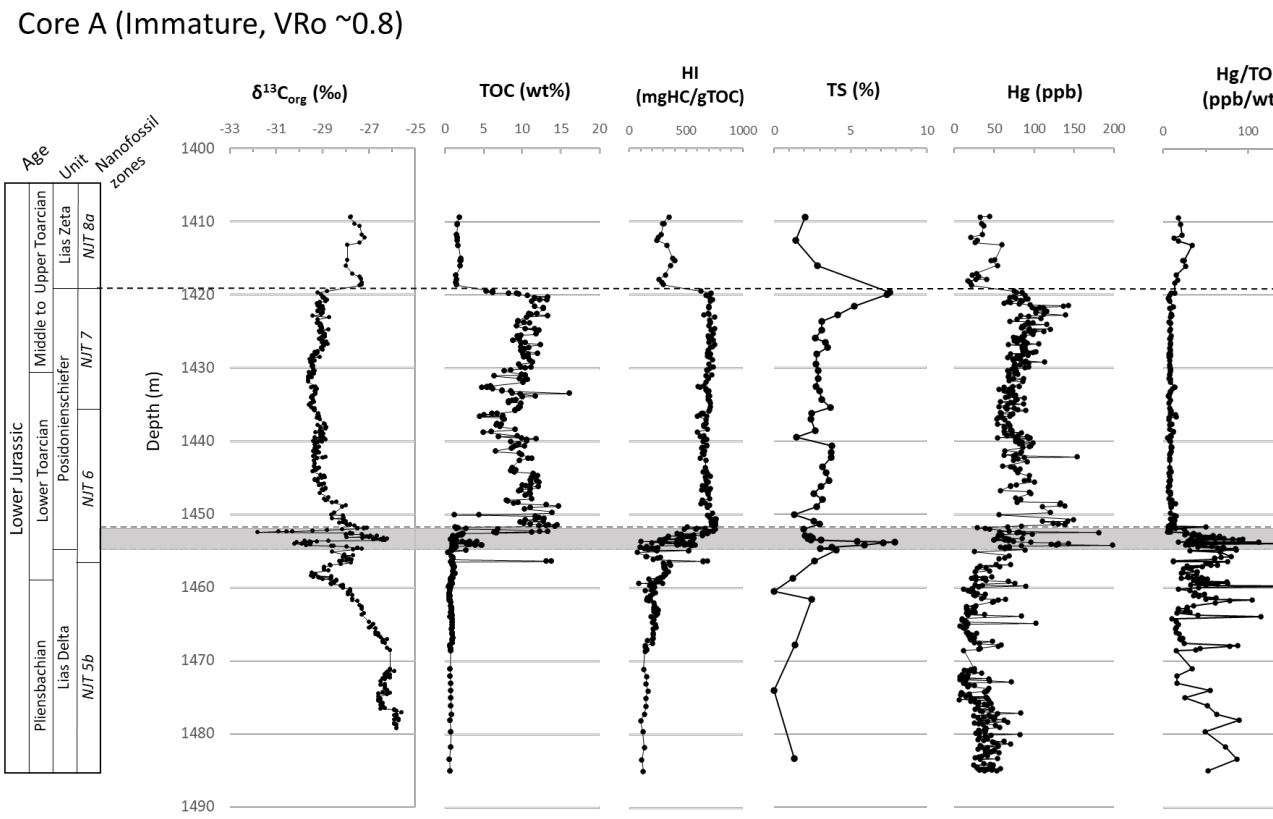

Figure 2. Stratigraphic log of the studied core A (immature, VRo ~0.8) showing ^{13}C data from bulk OM, the total organic carbon (TOC), hydrogen index (HI), total sulfur (TS), Hg content, Hg normalised by TOC, and Hg normalised by TS.

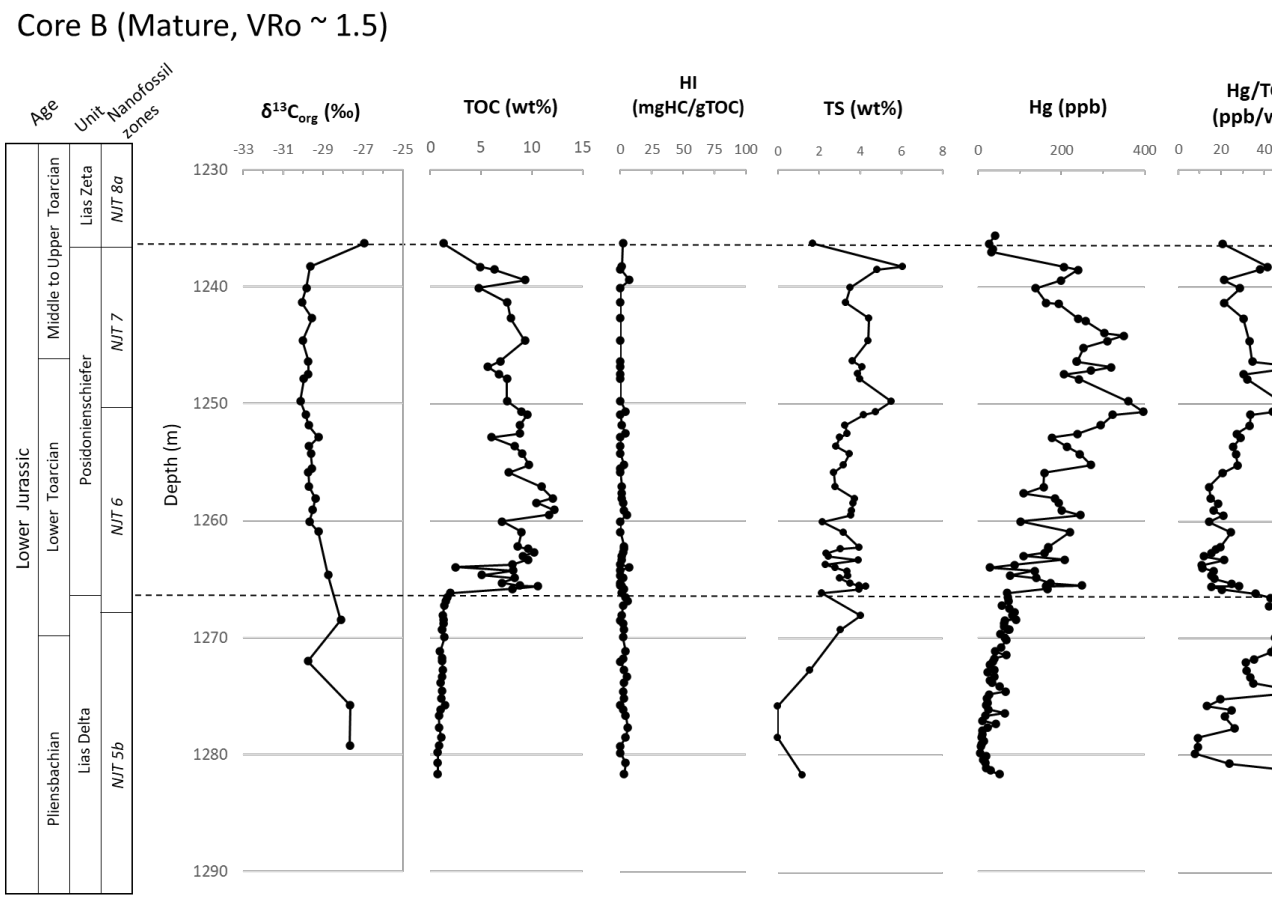

Figure 3. Stratigraphic log of the studied core B (mature, VRo ~1.5) showing ^{13}C data from bulk OM, the total organic carbon (TOC), hydrogen index (HI), total sulfur (TS), Hg content, Hg normalised by TOC, and Hg normalised by TS.

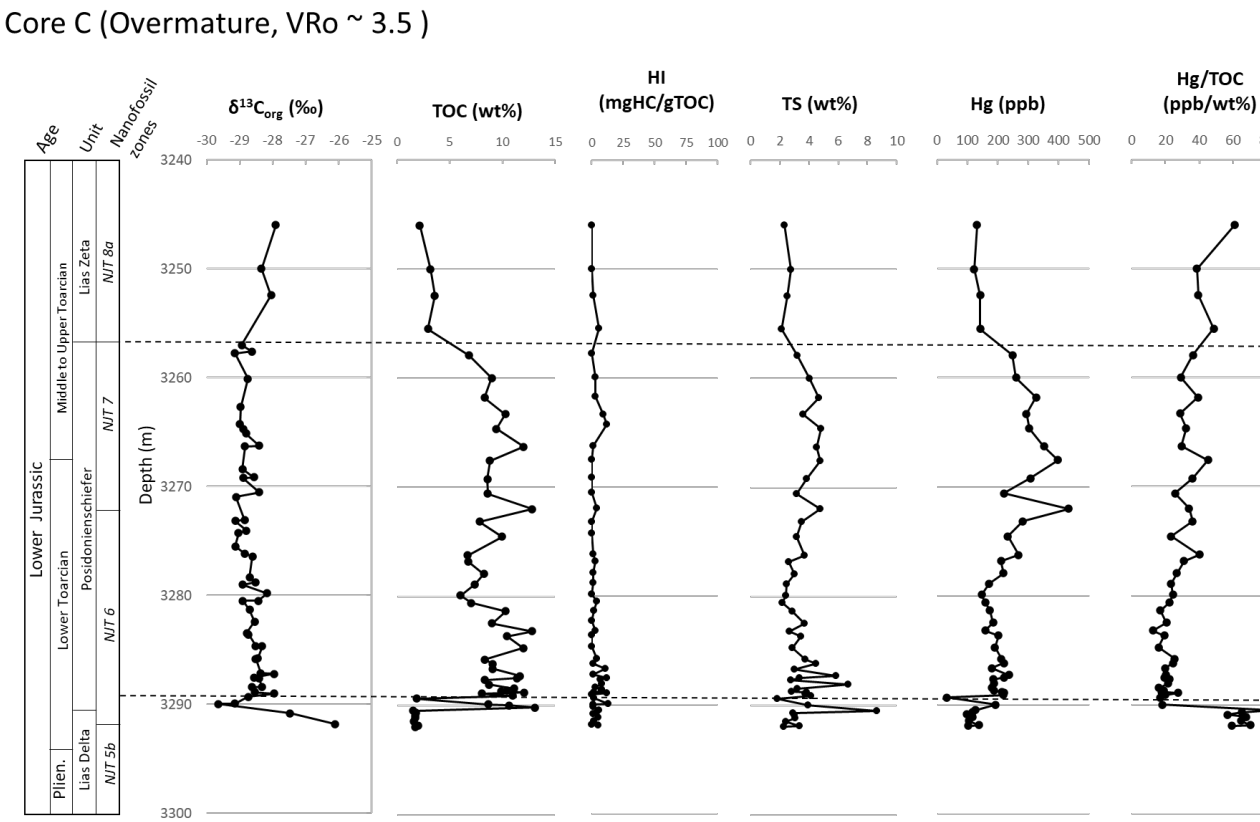

Figure 4. Stratigraphic log of the studied core C (overmature, VRo ~3.5) showing ^{13}C data from bulk OM, the total organic carbon (TOC), hydrogen index (HI), total sulfur (TS), Hg content, Hg normalised by TOC, and Hg normalised by TS.

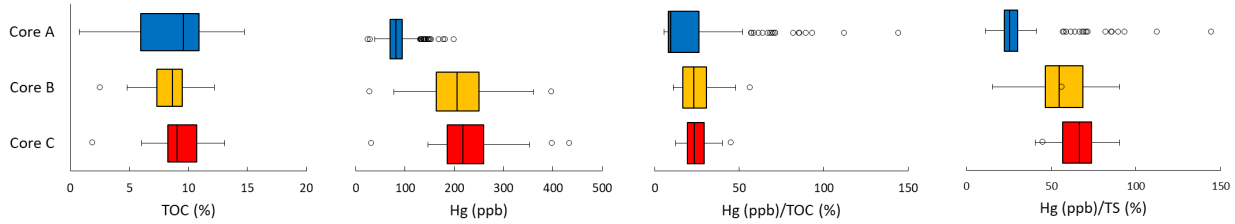

Figure 5. Differences between cores A, B and C in the mean (vertical lines), interquartile range (boxes) and data within 1.5 interquartile range (black lines with bar ends) of TOC (%), Hg (ppb), Hg/TOC (ppb/%), and Hg/TS (ppb/%) in the Posidonienschiefer.

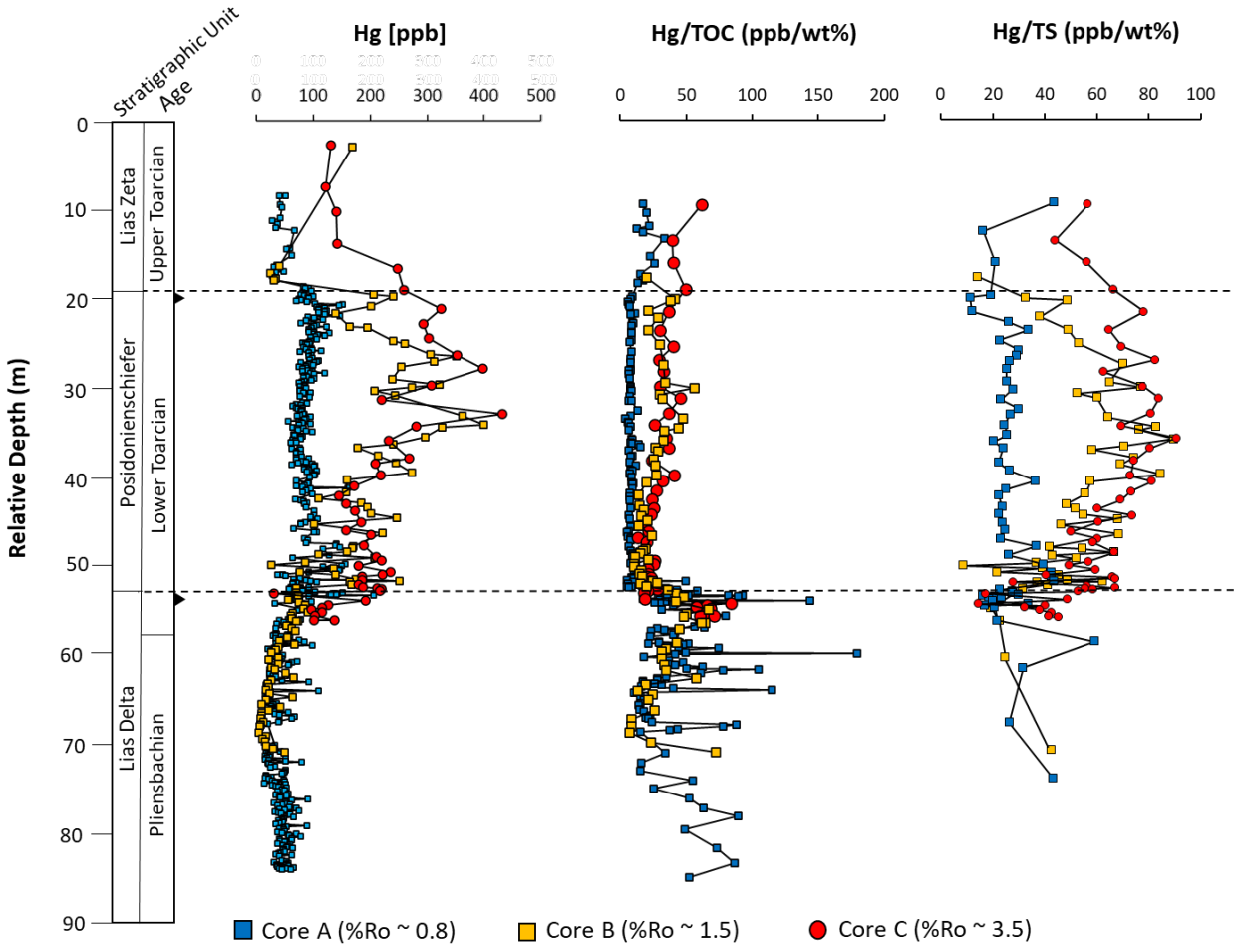

Figure 6. Hg contents, Hg/TOC, and Hg/TS in cores A, B, and C.

Table 1. TOC, Hg, TS, HI, OI and trace-metal data for cores A, B and C from the Posidonienschiefer. Symbols $^{+}$ indicate data from Hooker et al. (2020) and * from Dickson et al. (2022).

		Core		
		A	B	C
TOC	Mean	7.74	8.32	8.99
(%)	Std. Dev.	4.13	2.03	2.49
Hg	Mean	87.56	202.98	225.13
(ppb)	Std. Dev.	29.13	75.62	74.5
TS	Mean	3.47	3.59	3.73

		Core		
(%)	Std. Dev.	1.5	0.82	1.28
Hydrogen Index^{+}	Mean	589	2	3
(mgHC/gTOC)	Std. Dev.	155	2	4
Oxygen Index^{+}	Mean	21	19	13
($mgCO_2$/gTOC)	Std. Dev.	36	11	4
Cd*	Mean	1.7		1.8
(ppm)	Std. Dev.	1.1		0.6
Zn*	Mean	178		217
(ppm)	Std. Dev.	97		80
U*	Mean	5.7		16.1
(ppm)	Std. Dev.	2.4		11.8
Mo*	Mean	70.45		101.9
(ppm)	Std. Dev.	39.9		52.3

Table 2. Correlation between Hg, TOC, and TS for cores A, B and C from the Posidonienschiefer.

		Core		
		A	B	C
Hg-TOC	N	166	42	38
	R	0.309	0.254	0.427
	R^2	***0.096***	0.065	***0.182***
	p	***<0.001***	0.052	***0.004***
Hg-TS	N	48	41	38
	R	0.651	0.607	0.289
	R^2	***0.424***	***0.368***	***0.084***
	p	***<0.001***	***<0.001***	**0.039**
TS-TOC	N	48	41	38
	R	-0.086	-0.111	-0.07
	R^2	0.007	0.012	0.005
	p	0.28	0.246	0.338

Within the Posidonienschiefer, Hg content fluctuates between 53–154 ppb in core A (Fig. 2). In the equivalent interval of cores B and C, the range of Hg content is 28–397 ppb (Fig. 3) and 32–433 ppb (Fig. 4) respectively. The mean Hg content increases from 85 ppb (core A) to 203 ppb (B) and 225 ppb (C) (Table 1, Fig. 5). The Hg/TOC ratio in core A is in the range of 5–20 ppb/%, 10–56 ppb/% in core B, and 12–83 ppb/% in core C. The T-OAE-associated negative CIE is not clearly identifiable in cores B and C.

In core A, Hg/TOC ratios are very stable below 10 ppb/% throughout the Posidonienschiefer (Fig. 2), while in core B and core C, the Hg/TOC values

fluctuate more (Fig. 2, 3, and 4). The Hg/TOC ratios in core A diverge from those for cores B and C (Fig. 6). Above 50 m relative depth core A Hg/TOC is persistently lower (~10 ppb/%) compared to ~20 to 50 ppb/% for cores B and C. The Hg/TS ratio in core A is relatively stable throughout the Posidonienschiefer. Similar to the Hg/TOC signal, the Hg/TS signal in cores B and C diverges above 50 m relative depth from the core A Hg/TS signal (Fig. 6). The Hg/TS in cores B and C shows an increasing trend in the lower to the middle part of the section (max ~80-90 ppb/S%). The signal stabilises toward the top of the Posidonienschiefer in core B but decreases to 10 ppb/S% in core C (Fig. 6).

Correlations between Hg, TOC, and TS in the main high TOC sections are presented in Table 2. All individual correlations between Hg, TOC and TS explain less than 50% (R^2 <0.5) of the observed variance. With the exception of core B, Hg shows weak but significant (p <0.01) correlations with TOC. A similar relationship is found for TS, and Hg correlates significantly to TS in all cores. For core A and core B, Hg has stronger correlations with TS than with TOC. By contrast, Hg shows a very weak correlation with TS in core C and a weak correlation with TOC.

5. Discussion

5.1. Organic-matter characteristic of the Posidonienschiefer

In all three cores, Hg content in the Posidonienschiefer are higher than in the underlying Lias Zeta and overlying Lias Delta (Fig. 2, 3, and 4). The increased Hg content appear coincident with the much higher TOC in the Posidonienschiefer, a marked change from the marls and carbonate-dominated lithologies stratigraphically above and below, differences that reflect very pronounced changes in depositional redox conditions (Dickson et al., 2022). Within the Posidonienschiefer, the highest average TOC content is found in core C, followed by core B and core A (Table 1). This pattern is most likely a function of higher initial OM content in cores B and C, which, in turn, could be the result of their more distal position of the cores relative to the palaeo-shoreline (Dickson et al., 2022) and subdued siliciclastic input relative to supply of organic matter.

With HI values around 650–750 and oxygen index (OI) values under 20, the Posidonienschiefer can be interpreted as Type I/II kerogen showing a primary algal and amorphous organic-matter-dominated maceral assemblage (Littke et al., 1991). Algal-OM has shown high rates of Hg scavenging in modern lake and marine environments (Wallace, 1982; Zaferani et al., 2018; Outridge et al., 2019). Combined with the elevated TOC values (~5–15%), this interval can be identified as an excellent oil/gas-prone source-rock. Such sediments would undergo TOC breakdown when reaching burial temperature (50–150 °C), which, in turn, might affect Hg content and consequently Hg/TOC after the thermal maturation.

The stable TOC, HI and OI values within the Posidonienschiefer itself suggest only minor changes in the OM type, making the Posidonienschiefer ideal for studying the effects of thermal maturation on Hg contents and normalised Hg.

In contrast to core A, HI and OI values throughout cores B and C are extremely low throughout, consistent with the highly mature to post-mature stages of catagenesis experienced by the latter two cores (Tissot & Welte, 1984).

5.2. Mercury enrichment, carrier-phase depletion, or mobilisation in mature sediment?

We find that the average Hg content in the Posidonienschiefer is much higher in core B and core C compared to core A (Table 1, Fig. 5, 6). For the Posidonienschiefer, cores B and C have, on average, ~2.3–2.6-fold higher Hg content than core A. Assuming OM and sulfides were the dominant Hg carriers at the time of deposition, the elevated TOC influenced by the relative position of each core within the basin (see discussion §5.1) may have caused higher original Hg content in immature cores B and C. As can be seen in the divergent Hg and TOC- and S-normalised Hg, the most common carrier phases for Hg show a different signal compared to the element itself (Fig 6).

It is not possible to know exactly how much of the original organic-carbon content of the sediments has been lost during maturation. However, in an extreme scenario, up to ca. 60% of the original organic-carbon content of the sediments may have been lost during maturation (Lewan et al., 1979; Tissot & Welte, 1984; Raiswell & Berner, 1987). In turn, loss of organic carbon may have resulted in a significant (relative) enrichment in trace elements, if these were retained in the host rock. Hydrocarbon expulsion from the more mature cores thus potentially would have increased the relative trace-element concentrations through loss of mass. In addition to TOC loss, the removal water from the dehydration of clays during heating also likely contributed to the loss of rock mass (Peters & Cassa, 1994). A significant TOC loss will manifestly cause a more elevated value of normalised Hg/TOC in high-maturity OM-rich rocks (Fig. 5 and 6) if Hg is retained. This potentially results in a bias in both measured Hg and normalised Hg relative to the original signal stored in the rock record.

To assess whether mass loss or hydrocarbon expulsion processes have influenced the composition of our core material we compare our Hg data to previously published trace-element data. If the process of metal concentration due to loss of OM and water played a dominant role, the magnitude of change in Hg should resemble the relative increase in other (immobile) trace elements such as Mo, Zn, and Cd. Trace-metal increases observed between core A and core C did not exceed +45%, except for U (+185%; Table 1) (Dickson et al., 2020, 2022). The increase of +6 , +22, and +45% for Cd, Zn, and Mo concentrations, respectively from core A to C is primarily driven by TOC loss (up to ca. ~21%) during catagenesis, as demonstrated by Dickson et al. (2020) through pyrolysis experiments on the same core material.

The magnitude of change in Hg content compared to previously determined TOC loss (Dickson et al. 2020) shows that less than half the increase in Hg can be explained by mass loss during catagenesis. This implies that, in addition to the constant sum effects discussed above, other processes likely have played role.

Such processes could include, for example, internal redistribution of Hg in the sediment or capture of extraneous Hg within the Posidonienschiefer. Hg mobility during maturation might, for example, be attributed to volatility of weakly bound Hg^0 and Hg^{2+} at relatively low temperatures (60 to 225 °C) (Rumayor et al., 2013), which overlaps with catagenesis temperature experienced by this sequence in the Lower Saxony Basin (50 to 330 °C) (Bruns et al., 2013). In addition to the rise in average Hg content, its value is rather stable in core A, whereas an up-section increase is observed in cores B and C (Fig. 6). While this might be suggestive of Hg migration and (partial) recapture, this is difficult to envisage in lithologies such as the Posidonienschiefer that have extremely low matrix porosity and permeability, especially after burial to depths in excess of 8 km (Hooker et al., 2020).

An alternative explanation might be that the TOC, TS and Hg of core B and C were slightly higher in the upper interval at the time of deposition. Although the basin is generally characterised by euxinic conditions, the presumed greater palaeo-water depths of core B and C and thereby relative thicknesses of the euxinic water column may have resulted in slightly higher TOC, TS and Hg at the time of deposition.

From the correlation between Hg, TOC, and TS in Table 2., Hg correlates significantly with TOC and TS in all cores, without there being correlation between TOC and TS. The relationship indicates the tendency of Hg likely being hosted in both the organic C fraction and sulfur compounds which add complexity to the mechanism of redistribution/re-capture of Hg during thermal maturation.

5.3. Potential mechanisms of perceived Hg enrichment: fractures, and fluid (hydrocarbon) migration or different starting conditions?

The maturation of organic matter and heating of sediments ultimately can lead to fluid overpressures and fracturing of low-porosity/permeability rocks. For example, according to Meissner (1978), the catagenesis of solid kerogen into liquid hydrocarbons, gas, residue and other by-products is accompanied by a volume expansion of up to 25%. It has been suggested that this volume-change reaction would increase local fluid pressures resulting in hydraulic fracturing and formations of veins (e.g., Mandl & Harkness, 1987; Lash & Engelder, 2005). Shale layers in cores B and C contain abundant layer-parallel and oblique veins, mostly filled by calcite cement, with traces of pyrite crystals (Hooker et al., 2020). These oblique and bedding-parallel fractures containing so-called 'beef' calcite may have played an important role in the primary migration of petroleum fluids within and from the Posidonienschiefer (Leythaeuser et al., 1988), but, as Hooker et al. (2020) indicate, the potential for vertical migration through the fractures that are filled with calcite is low, as well as the postulated porosity and permeability within the fracture fill. Whether large-scale fractures or networks of fractures existed outside the cored interval and facilitated fluid migration cannot be established with the present material.

Alternatively, core B and C may have had slightly higher Hg during deposition, due to their higher TOC content. However, if we assume that Hg/TOC of the immature core (~11 ppb/%) is representative of the original Hg/TOC of cores B and C and that Hg in these cores did not change, the TOC loss in those cores would need to be ~45% to reach the observed Hg content. A loss of 45% far exceeds the observed TOC loss during pyrolysis experiments (21%, Dickson et al. 2020) and is inconsistent with enrichments other trace element data. This implies that, if starting conditions were different, Hg/TOC for cores B and C should have been substantially higher than for core A. Such higher Hg/TOC and Hg/TS seems unlikely given their distal position in the basin and greater potential for strongly reducing conditions, which typically lead to reduced, not increased, Hg/TOC and Hg/TS (Them et al., 2019; Grasby et al., 2019; Shen et al., 2022; Frieling et al., in review).

5.4. Implications for the use of the Hg proxy in mature sediments

For the compiled data of Grasby et al. (2019) that includes both background and events with active LIPs, average shale values of 62.4 ppb and 71.9 ppb/%TOC are given. The "peak" of Hg contents (397 ppb and 433 ppb) in mature cores B and C (Fig. 3 and 4) are in the range of "Hg spikes" in the geological record previously interpreted to result from LIP activity (e.g., ~20 ppb Hg, associated with the Early Cretaceous Greater Ontong Java LIP (Charbonnier & Föllmi, 2017) to 2517 ppb Hg at the Frasnian–Famennian (Devonian) transition (Racki et al., 2018)). However, the TOC-normalised Hg in the two mature cores (56 ppb/% and 48 ppb/ %) are not in the range of recorded Hg/TOC generally considered as volcanic peaks (e.g., ~175 ppb/ % at the Greater Ontong Java LIP and 7102 ppb/ % at the Frasnian-Famennian transition). The Hg peaks in cores B and C (397-433 ppb) likely resulted from Hg redistribution and rock mass loss during thermal maturation, yet the maximum Hg content is similar to the peak Hg anomaly in Siberian Traps (396 ppb) (Wang et al., 2018) and Deccan Traps (415 ppb) (Sial et al., 2013).

The divergence of the Hg/TOC and Hg/TS above 50 m relative depth (Fig. 6) in cores B and C from a stable signal of Hg/TOC and Hg/TS in core A is difficult to explain without a degree of Hg redistribution and/or slightly higher Hg for the upper Posidonienschiefer in core B and C (see section 5.3). Regardless of the mechanism, the increase in Hg/TOC from TOC alone implies knowledge of thermal maturation history of the material becomes critical for the interpretation of Hg records when analysing sediments that have been exposed to significant temperatures. For example, if the elevated Hg/TOC in core B and C were to be interpreted without the context of core A and associated thermal maturity data, it might be interpreted as increased Hg loading or variability at the time of deposition. It is obvious from our findings that data from successions with significant calcite veins from hydrocarbon migration or other high-temperature fluid migration, similar to those observed in the Posidonienschiefer should be treated with extreme caution. Lastly, we cannot exclude that veins formed during, for example, (non-thermal) fluid escape could have served as similar

pathways for Hg redistribution.

Thermally mature sediments have been previously used to assess the potential role of volcanic Hg enrichment in the T-OAE (e.g., East Tributary and core 1-35-62-5W6 (Canada) with Tmax > 450 °C shows peak Hg/TOC of 58 ppb/% and 28 ppb/% respectively (Them et al., 2019), which is in the range of Hg/TOC found in cores B and C). However, if in fact the mercury content increased simultaneously with the loss of TOC during thermal maturation, as suggested by our results here, it could imply that the Hg and Hg/TOC in these more mature and overmature Canadian cores might overestimate Hg loading compared to immature sections elsewhere. When comparing the Canadian T-OAE core material to other T-OAE sections (e.g., Bornholm, Denmark section with Hg/TOC 2590 ppb/% (Percival et al., 2015) and El Peñon, Chile with Hg/TOC 234 ppb/% (Fantasia et al., 2018)), there is no tell-tale sign they are systemically biased. This is likely because the increase in (normalised) Hg introduced by thermal maturation is small relative to the local and (supra)regional variability in Hg deposition (Lepland et al., 2010; Leipe et al., 2013; Percival et al., 2018; Them et al., 2019) and would likely go unnoticed unless the effects of burial-related heating can be isolated, as we have done here. For periods when all records are thermally mature as would be progressively more likely with sediment deposited further back in time, systematic increases in Hg and normalised Hg with thermal maturity could lead to overestimated volcanic (Hg) emissions.

6. Conclusions

We studied three cores spanning the same formation with different levels of thermal maturity from the Lower Toarcian Posidonienschiefer in the Lower Saxony Basin, Germany. We show the increases of Hg content in mature core B and overmature core C were as high as +132% to +157% relative to the immature core A. Because thermal maturation also reduced the TOC content of the host rock at high levels of maturity, Hg/TOC ratios from mature sediments are considerably inflated. Consequently, the use of Hg and Hg/TOC ratios in mature organic-rich shale could lead to overestimates of Hg inventories in the geological past. Further, the magnitude of Hg enrichment is much larger than observed for other trace metals (e.g., Mo, Cd, Zn), which implies that the loss of mass caused by expulsion of hydrocarbons as a result of thermal maturation might not be the only process involved in causing elevated Hg content.

Mature cores B and C showed high Hg content variability profile in contrasts with the relatively stable Hg content profile in core A. We argue that the pronounced difference in the stratigraphic signals might be explained by the mobility and volatility of Hg in the temperature range of thermal maturation in the LSB, the precise mechanisms of mobilisation and re-sequestration remain elusive. Specifically, the observed fractures in cores B and C may have allowed Hg to migrate and re-adsorb at key levels in the stratigraphy, although there is still large uncertainty how this would effectively permeate the bulk of the lithology due to the extremely low matrix porosity and permeability of the Posidonienschiefer.

In general, the magnitude of elevated Hg content and TOC-normalised Hg in the mature cores (B and C) found here is not as high as Hg peak values interpreted as mercury perturbations caused by LIP volcanism. Nonetheless, our results show that the thermal history of sediments must be considered when using Hg as a proxy for volcanism. Specifically, the >2-fold enrichment in Hg content associated with maturation and the potential influence of fluid migration leading to levels of relative Hg enrichment warrant a cautious approach when using (over)mature and especially fractured sedimentary successions as an archive for far-field subaerial volcanic activity.

Hg mobilization processes during thermal maturation, hydrocarbon expulsion and migration history should be considered in evaluating Hg in oil and gas reservoirs. It is essential not only to think about Hg content in the original immature source rock but also how sediment thermal maturity level might enrich or, oppositely, reduce Hg content in the final product

Acknowledgments

We thank S. Wyatt (University of Oxford) and J. Brakeley (Royal Holloway University of London) for analytical assistance. Funding was provided from European Research Council Consolidator Grant (ERC-2018-COG-818717-V-ECHO). Special thanks to Shell Global Solutions B.V. for access to samples for this study. A.I. is supported by a Jardine Foundation scholarship.

Data Availability Statement

All newly generated data will be made available through a permanent online data repository upon publication.

References

Abarghani, A., Gentzis, T., Liu, B., Khatibi, S., Bubach, B., & Ostadhassan, M. (2020). Preliminary investigation of the effects of thermal maturity on redox-sensitive trace metal concentration in the Bakken source rock, North Dakota,. *American Chemical Society Omega*, *5*(13), 7135–7148. https://doi.org/10.1021/acsomega.9b03467

Behar, F., Beaumont, V., & De B. Penteado, H. L. (2001). Rock-Eval 6 technology: performances and developments. *Oil & Gas Science and Technology*, *56*(2), 111–134. https://doi.org/10.2516/ogst:2001013

Benoit, J. M., Mason, R. P., Gilmour, C. C., & Aiken, G. R. (2001). Constants for mercury binding by organic matter isolates from the Florida Everglades. *Geochimica et Cosmochimica Acta*, *65*(24), 4445–4451. https://doi.org/10.1016/S0016-7037(01)00742-6

Betz, D., Führer, F., Greiner, G., & Plein, E. (1987). Evolution of the Lower Saxony Basin. *Tectonophysics*, *137*(1–4). https://doi.org/10.1016/0040-1951(87)90319-2

Bin, C., Xiaoru, W., & Lee, F. S. C. (2001). Pyrolysis coupled with atomic

absorption spectrometry for the determination of mercury in Chinese medicinal materials. *Analytica Chimica Acta*, *447*(1–2), 161–169. https://doi.org/10.1016/S0003-2670(01)01218-1

Blumenberg, M., Zink, K. G., Scheeder, G., Ostertag-Henning, C., & Erbacher, J. (2019). Biomarker paleo-reconstruction of the German Wealden (Berriasian, Early Cretaceous) in the Lower Saxony Basin (LSB). *International Journal of Earth Sciences, 108,* 229–244. https://doi.org/10.1007/s00531-018-1651-5

Brink, H. J., Dürschner, H., & Trappe, H. (1992). Some aspects of the late and post-Variscan development of the Northwestern German Basin. *Tectonophysics*, *207*(1–2), 65–95. https://doi.org/10.1016/0040-1951(92)90472-I

Bruns, B., di Primio, R., Berner, U., & Littke, R. (2013). Petroleum system evolution in the inverted Lower Saxony Basin, northwest Germany: A 3D basin modeling study. *Geofluids*, *13*(2), 246–271. https://doi.org/10.1111/gfl.12016

Carvajal-Ortiz, H., Gentzis, T., & Ostadhassan, M. (2021). Sulfur differentiation in organic-rich shales and carbonates via open-system programmed pyrolysis and oxidation: insights into fluid souring and H_2S production in the Bakken Shale, United States. *Energy and Fuels*, *35*(15), 12030–12044. https://doi.org/10.1021/acs.energyfuels.1c01562

Chappaz, A., Lyons, T. W., Gregory, D. D., Reinhard, C. T., Gill, B. C., Li, C., & Large, R. R. (2014). Does pyrite act as an important host for molybdenum in modern and ancient euxinic sediments? *Geochimica et Cosmochimica Acta*, *126*, 112–122. https://doi.org/10.1016/j.gca.2013.10.028

Charbonnier, G., & Föllmi, K. B. (2017). Mercury enrichments in lower Aptian sediments support the link between Ontong Java large igneous province activity and oceanic anoxic episode 1a. *Geology*, *45*(1), 63–66. https://doi.org/10.1130/G38207.1

Dahl, T. W., Chappaz, A., Hoek, J., McKenzie, C. J., Svane, S., & Canfield, D. E. (2017). Evidence of molybdenum association with particulate organic matter under sulfidic conditions. *Geobiology*, *15*(2), 311–323. https://doi.org/10.1111/gbi.12220

Dickson, A. J., Idiz, E., Porcelli, D., & van den Boorn, S. H. J. M. (2020). The influence of thermal maturity on the stable isotope compositions and concentrations of molybdenum, zinc and cadmium in organic-rich marine mudrocks. *Geochimica et Cosmochimica Acta*, *287*, 205–220. https://doi.org/10.1016/j.gca.2019.11.001

Dickson, A. J., Idiz, E., Porcelli, D., Murphy, M. J., Celestino, R., Jenkyns, H. C., et al. (2022). No effect of thermal maturity on the Mo, U, Cd, and Zn isotope compositions of Lower Jurassic organic-rich sediments. *Geology*, *50*(5), 598–602. https://doi.org/10.1130/g49724.1

Fadeeva, V. P., Tikhova, V. D., & Nikulicheva, O. N. (2008). Elemental analysis of organic compounds with the use of automated

CHNS analyzers. *Journal of Analytical Chemistry*, *63*(11), 1094–1106. https://doi.org/10.1134/S1061934808110142

Fantasia, A., Föllmi, K. B., Adatte, T., Bernárdez, E., Spangenberg, J. E., & Mattioli, E. (2018). The Toarcian oceanic anoxic event in southwestern Gondwana: An example from the Andean Basin, northern Chile. *Journal of the Geological Society*, *175*(6), 883–902. https://doi.org/10.1144/jgs2018-008

French, K.L., Sepúlveda, J., Trabucho-Alexandre, J., Gröcke, D.R., & Summons, R.E. (2014). Organic geochemistry of the early Toarcian oceanic anoxic event in Hawsker Bottoms, Yorkshire, England. *Earth and Planetary Science Letters*, *390*, 116-127. https://doi.org/10.1016/j.epsl.2013.12.033

Frieling J., Mather T. A., März C., Jenkyns H. C., Hennekam R., Reichart G., Slomp C. P., & van Helmond N. A. G. M. (2022). Effects of redox variability and early diagenesis on marine sedimentary Hg records. ESSOAr. Preprint. https://doi.org/10.1002/essoar.10512647.1

Celestino, R. (2019). Environmental change and carbon cycling during the Early Jurassic : A multi-proxy study on the Posidonienschiefer of NW Germany, (Doctoral dissertation). (http://hdl.handle.net/10871/36576). Exeter, UK. University of Exeter.

Fitzgerald, W. F., Lamborg, C. H., & Hammerschmidt, C. R. (2007). Marine biogeochemical cycling of mercury. *Chemical Reviews*, *107*(2), 641–662. https://doi.org/10.1021/cr050353m

Frimmel, A., Oschmann, W., & Schwark, L. (2004). Chemostratigraphy of the Posidonia Black Shale, SW Germany I. Influence of sea-level variation on organic facies evolution. *Chemical Geology*, *206*(3–4), 199–230. https://doi.org/10.1016/j.chemgeo.2003.12.007

Gajdosechova, Z., Boskamp, M. S., Lopez-Linares, F., Feldmann, J., & Krupp, E. M. (2016). Hg speciation in petroleum hydrocarbons with emphasis on the reactivity of Hg particles. *Energy and Fuels*, *30*(1), 130–137. https://doi.org/10.1021/acs.energyfuels.5b02080

Gehrke, G. E., Blum, J. D., & Meyers, P. A. (2009). The geochemical behavior and isotopic composition of Hg in a mid-Pleistocene western Mediterranean sapropel. *Geochimica et Cosmochimica Acta*, *73*(6), 1651–1665. https://doi.org/10.1016/j.gca.2008.12.012

Grasby, S. E., Shen, W., Yin, R., Gleason, J. D., Blum, J. D., Lepak, R. F., et al. (2017). Isotopic signatures of mercury contamination in latest Permian oceans. *Geology*, *45*(1), 55–58. https://doi.org/10.1130/G38487.1

Grasby, S. E., Them, T. R., Chen, Z., Yin, R., & Ardakani, O. H. (2019). Mercury as a proxy for volcanic emissions in the geologic record. *Earth-Science Reviews*, *196*(March), 102880. https://doi.org/10.1016/j.earscirev.2019.102880

Hooker, J. N., Ruhl, M., Dickson, A. J., Hansen, L. N., Idiz, E., Hesselbo, S.

P., & Cartwright, J. (2020). Shale anisotropy and natural hydraulic fracture propagation: An example from the Jurassic (Toarcian) Posidonienschiefer, Germany. *Journal of Geophysical Research: Solid Earth*, *125*(3), 1–14. https://doi.org/10.1029/2019JB018442

Jenkyns, H. C. (1985). The Early Toarcian and Cenomanian-Turonian anoxic events in Europe: comparisons and contrasts. *Geologische Rundschau, 74*(3), 505-518. https://doi.org/10.1007/BF01821208

Jenkyns, H. C. (1988). The early Toarcian (Jurassic) anoxic event; stratigraphic, sedimentary and geochemical evidence. *American Journal of Science*, *288*(2), 101-151. https://doi.org/10.2475/ajs.288.2.101

Jones, M. T., Percival, L. M. E., Stokke, E. W., Frieling, J., Mather, T. A., Riber, L., et al. (2019). Mercury anomalies across the Palaeocene-Eocene Thermal Maximum. *Climate of the Past*, *15*(1), 217–236. https://doi.org/10.5194/cp-15-217-2019

Krupp, R. (1988). Physicochemical aspects of mercury metallogenesis. *Chemical Geology*, *69*(3–4), 345–356. https://doi.org/10.1016/0009-2541(88)90045-9

Lamborg, C. H., Fitzgerald, W. F., Damman, A. W. H., Benoit, J. M., Balcom, P. H., & Engstrom, D. R. (2002a). Modern and historic atmospheric mercury fluxes in both hemispheres: Global and regional mercury cycling implications. *Global Biogeochemical Cycles*, *16*(4), 1104. https://doi.org/10.1029/2001gb001847

Lamborg, C. H., Fitzgerald, W. F., O'Donnell, J., & Torgersen, T. (2002b). A non-steady-state compartmental model of global-scale mercury biogeochemistry with interhemispheric atmospheric gradients. *Geochimica et Cosmochimica Acta*, *66*(7), 1105–1118. https://doi.org/10.1016/S0016-7037(01)00841-9

Lash, G. G., & Engelder, T. (2005). An analysis of horizontal microcracking during catagenesis: Example from the Catskill delta complex. *American Association of Petroleum Geologists Bulletin*, *89*(11), 1433–1449. https://doi.org/10.1306/05250504141

Leipe, T., Moros, M., Kotilainen, A., Vallius, H., Kabel, K., Endler, M., & Kowalski, N. (2013). Mercury in Baltic Sea sediments - Natural background and anthropogenic impact. *Geochemistry*, *73*(3), 249–259. https://doi.org/10.1016/j.chemer.2013.06.005

Lepland, A., Andersen, T. J., Lepland, A., Arp, H. P. H., Alve, E., Breedveld, G. D., & Rindby, A. (2010). Sedimentation and chronology of heavy metal pollution in Oslo harbor, Norway. *Marine Pollution Bulletin*, *60*(9), 1512–1522. https://doi.org/10.1016/j.marpolbul.2010.04.017

Lewan, M. D., Winters, J. C., & Mcdonald, J. H. (1979). Generation of oil-like pyrolyzates from organic-rich shales. *Science, 203*(4383), 897–899. http://www.jstor.org/stable/1747886

Lewan, M. D., & Maynard, J. (1982). Factors controlling enrichment of vanadium and nickel in the bitumen of organic sedimentary rocks. *Geochimica et Cosmochimica Acta*, *46*(12), 2547–2560. https://doi.org/10.1016/0016-7037(82)90377-5

Leythaeuser, D., Littke, R., Radke, M., & Schaefer, R. G. (1988). Geochemical effects of petroleum migration and expulsion from Toarcian source rocks in the Hils syncline area, NW-Germany. *Organic Geochemistry*, *13*(1–3), 489–502. https://doi.org/10.1016/0146-6380(88)90070-8

Lindqvist, O., Johansson, K., Bringmark, L., Timm, B., Aastrup, M., Andersson, A., et al. (1991). Mercury in the Swedish environment - Recent research on causes, consequences and corrective methods. *Water, Air, & Soil Pollution*, *55*(1–2). https://doi.org/10.1007/BF00542429

Littke, R., Baker, D. R., & Leythaeuser, D. (1988). Microscopic and sedimentologic evidence for the generation and migration of hydrocarbons in Toarcian source rocks of different maturities. *Organic Geochemistry*, *13*(1–3), 549–559. https://doi.org/10.1016/0146-6380(88)90075-7

Littke, R., Leythaeuser, D., Rullkötter, J., & Baker, D. R. (1991). Keys to the depositional history of the Posidonia Shale (Toarcian) in the Hils Syncline, northern Germany. *Geological Society Special Publication*, *58*(58), 311–333. https://doi.org/10.1144/GSL.SP.1991.058.01.20

Liu Z., Tian H., Yin R., Chen D., & Gai H. (2022) Mercury loss and isotope fractionation during thermal maturation of organic-rich mudrocks. *Chemical Geology*, *612*, 121144. https://doi.org/10.1016/j.chemgeo.2022.121144

Mandl, G., & Harkness, R. M. (1987). Hydrocarbon migration by hydraulic fracturing. *Geological Society Special Publication*, *29*, 39–53. https://doi.org/10.1144/GSL.SP.1987.029.01.04

Mason, R. P., Fitzgerald, W. F., & Morel, F. M. M. (1994). The biogeochemical cycling of elemental mercury: Anthropogenic influences. *Geochimica et Cosmochimica Acta*, *58*(15), 3191–3198. https://doi.org/10.1016/0016-7037(94)90046-9

Meissner, F. F. (1978). Petroleum geology of the Bakken formation Williston basin, North Dakota and Montana. In D. Estelle, R. Miller (Eds.), *Montana Geological Society: 24th Annual Conference: 1978 Williston Basin Symposium* (pp. 207-227). Billings, MT: Montana Geological Society.

Mukherjee, A. B., Bhattacharya, P., Sarkar, A., & Zevenhoven, R. (2009). Mercury emissions from industrial sources in India and its effects in the environment. In R. Mason & N. Pirrone (Eds.), *Mercury fate and transport in the global atmosphere: Emissions, measurements and models* (pp. 81–112). Boston, MA: Springer US. https://doi.org/10.1007/978-0-387-93958-2_4

Outridge, P. M., Sanei, H., Stern, G. A., Hamilton, P. B., & Goodarzi, F. (2007). Evidence for control of mercury accumulation rates in Canadian High Arctic

Lake sediments by variations of aquatic primary productivity. *Environmental Science and Technology*, *41*(15), 5259–5265. https://doi.org/10.1021/es070408x

Outridge, P. M., Stern, G. A., Hamilton, P. B., & Sanei, H. (2019). Algal scavenging of mercury in preindustrial Arctic lakes. *Limnology and Oceanography*, *64*(4), 1558–1571. https://doi.org/10.1002/lno.11135

Percival, L. M. E., Bergquist, B. A., Mather, T. A., & Sanei, H. (2021). Sedimentary mercury enrichments as a tracer of large igneous province volcanism. In R.E. Ernst, A.J. Dickson and A. Bekker (Eds.), *Large igneous provinces: A driver of global environmental and biotic changes, Geophysical Monograph Series* (Vol. 255, pp. 247–262). Washington, DC and Hoboken, NJ: American Geophysical Union and John Wiley and Sons, Inc. https://doi.org/10.1002/9781119507444.ch11

Percival, L. M. E., Witt, M. L. I., Mather, T. A., Hermoso, M., Jenkyns, H. C., Hesselbo, S. P., et al. (2015). Globally enhanced mercury deposition during the end-Pliensbachian extinction and Toarcian OAE : A link to the Karoo – Ferrar Large Igneous Province. *Earth and Planetary Science Letters*, *428*, 267–280. https://doi.org/http://dx.doi.org/10.1016/j.epsl.2015.06.064

Percival, L. M. E., Jenkyns, H. C., Mather, T. A., Dickson, A. J., Batenburg, S. J., Ruhl, M., et al. (2018). Does large igneous province volcanism always perturb the mercury cycle? Comparing the records of Oceanic Anoxic Event 2 and the end-Cretaceous to other Mesozoic events. *American Journal of Science*, *318*(8), 799–860. https://doi.org/10.2475/08.2018.01

Peters, K. E., & Cassa, M. R. (1994). Applied source rock geochemistry. In L.B. Magoon, W.G. Dow (Eds.), *The petroleum system—from source to trap*, *American Association of Petroleum Geologists Memoir* (Vol. 60, pp 93–120). Tulsa, OK: The American Association of Petroleum Geologists.

Pyle, D. M., & Mather, T. A. (2003). The importance of volcanic emissions for the global atmospheric mercury cycle. *Atmospheric Environment*, *37*(36), 5115–5124. https://doi.org/10.1016/j.atmosenv.2003.07.011

Racki, G., Rakocinski, M., Marynowski, L., & Wignall, P. B. (2018). Mercury enrichments and the Frasnian-Famennian biotic crisis: A volcanic trigger proved? *Geology*, *46*(6), 543–546. https://doi.org/10.1130/G40233.1

Raiswell, R., & Berner, R. A. (1987). Organic carbon losses during burial and thermal maturation of normal marine shales. *Geology*, *15*(9), 853–856. https://doi.org/10.1130/0091-7613(1987)15<853:OCLDBA>2.0.CO;2

Riegraf, W., Werner, G., & Lörcher, F. (1984). Der Posidonienschiefer: Biostratigraphie, Fauna und Fazies des südwestdeutschen Untertoarciums (Lias Epsilon). Stuttgart: F. Enke, 195pp.

Röhl, H. J., Schmid-Röhl, A., Oschmann, W., Frimmel, A., & Schwark, L. (2001). The Posidonia Shale (Lower Toarcian) of SW-Germany:

An oxygen-depleted ecosystem controlled by sea level and palaeoclimate. *Palaeogeography, Palaeoclimatology, Palaeoecology*, *165*(1–2), 27–52. https://doi.org/10.1016/S0031-0182(00)00152-8

Rullkötter, J., Leythaeuser, D., Horsfield, B., Littke, R., Mann, U., Müller, P. J., et al. (1988). Organic matter maturation under the influence of a deep intrusive heat source: A natural experiment for quantitation of hydrocarbon generation and expulsion from a petroleum source rock (Toarcian shale, northern Germany). *Organic Geochemistry*, *13*(4–6), 847–856. https://doi.org/10.1016/0146-6380(88)90237-9

Rullkötter, Jürgen, & Marzi, R. (1988). Natural and artificial maturation of biological markers in a Toarcian shale from northern Germany. *Organic Geochemistry*, *13*(4–6), 639–645. https://doi.org/10.1016/0146-6380(88)90084-8

Rumayor, M., Diaz-Somoano, M., Lopez-Anton, M. A., & Martinez-Tarazona, M. R. (2013). Mercury compounds characterization by thermal desorption. *Talanta*, *114*, 318–322. https://doi.org/10.1016/j.talanta.2013.05.059

Sanei, H. (2020). Genesis of solid bitumen. *Scientific Reports*, *10*(1), 1–10. https://doi.org/10.1038/s41598-020-72692-2

Sanei, H., Grasby, S. E., & Beauchamp, B. (2012). Latest Permian mercury anomalies. *Geology*, *40*(1), 63–66. https://doi.org/10.1130/G32596.1

Scaife, J. D., Ruhl, M., Dickson, A. J., Mather, T. A., Jenkyns, H. C., Percival, L. M. E., et al. (2017). Sedimentary Mercury Enrichments as a Marker for Submarine Large Igneous Province Volcanism? Evidence From the Mid-Cenomanian Event and Oceanic Anoxic Event 2 (Late Cretaceous). *Geochemistry, Geophysics, Geosystems*, *18*(12), 4253–4275. https://doi.org/10.1002/2017GC007153

Schmid-Röhl, A., Röhl, H. J., Oschmann, W., Frimmel, A., & Schwark, L. (2002). Palaeoenvironmental reconstruction of Lower Toarcian epicontinental black shales (Posidonia Shale, SW Germany): Global versus regional control. *Geobios*, *35*(1), 13–20. https://doi.org/10.1016/S0016-6995(02)00005-0

Schwark, L., & Frimmel, A. (2004). Chemostratigraphy of the Posidonia Black Shale, SW-Germany II. Assessment of extent and persistence of photic-zone anoxia using aryl isoprenoid distributions. *Chemical Geology*, *206*(3–4), 231–248. https://doi.org/10.1016/j.chemgeo.2003.12.008

Shen, J., Feng, Q., Algeo, T. J., Liu, J., Zhou, C., Wei, W., et al. (2020). Sedimentary host phases of mercury (Hg) and implications for use of Hg as a volcanic proxy. *Earth and Planetary Science Letters*, *543*, 116333. https://doi.org/10.1016/j.epsl.2020.116333

Shen, J., Algeo, T.J., & Feng, Q. (2022). Mercury isotope evidence for a non-volcanic origin of Hg spikes at the Ordovician-Silurian boundary, South China. *Earth and Planetary Science Letters, 594*, 117705. https://doi.org/10.1016/j.epsl.2022.117705

Sial, A. N., Lacerda, L. D., Ferreira, V. P., Frei, R., Marquillas, R. A., Barbosa, J. A., et al. (2013). Mercury as a proxy for volcanic activity during extreme environmental turnover : The Cretaceous – Paleogene transition. *Palaeogeography, Palaeoclimatology, Palaeoecology*, *387*, 153–164. https://doi.org/10.1016/j.palaeo.2013.07.019

Song, J., Littke, R., & Weniger, P. (2017). Organic geochemistry of the Lower Toarcian Posidonia Shale in NW Europe. *Organic Geochemistry*, *106*, 76-92. https://doi.org/10.1016/j.orggeochem.2016.10.014

Them, T. R., Jagoe, C. H., Caruthers, A. H., Gill, B. C., Grasby, S. E., Gröcke, D. R., et al. (2019). Terrestrial sources as the primary delivery mechanism of mercury to the oceans across the Toarcian Oceanic Anoxic Event (Early Jurassic). *Earth and Planetary Science Letters*, *507*, 62–72. https://doi.org/10.1016/j.epsl.2018.11.029

Tissot, B. P., & Welte, D. H. (1984). Sedimentary processes and the accumulation of organic matter. In Tissot, B.P., Welte, D.H., *Petroleum Formation and Occurrence* (pp. 55–62). Berlin: Springer-Verlag. https://doi.org/10.1007/978-3-642-96446-6_5

UN Environment. (2019). *Global Mercury Assessment 2018*. UN Environment Programme, Chemicals and Health Branch Geneva, Switzerland.

Wallace, G. T. (1982). The association of copper, mercury and lead with surface-active organic matter in coastal seawater. *Marine Chemistry*, *11*(4), 379–394. article. https://doi.org/10.1016/0304-4203(82)90032-9

Wang, X., Cawood, P. A., Zhao, H., Zhao, L., Grasby, S. E., Chen, Z. Q., et al. (2018). Mercury anomalies across the end Permian mass extinction in South China from shallow and deep water depositional environments. *Earth and Planetary Science Letters*, *496*, 159–167. https://doi.org/10.1016/j.epsl.2018.05.044

Wang, Z., Tan, J., Boyle, R., Wang, W., Kang, X., Dick, J., & Lyu, Q. (2020). Mercury anomalies within the lower Cambrian (stage 2–3) in South China: Links between volcanic events and paleoecology. *Palaeogeography, Palaeoclimatology, Palaeoecology*, *558*(April). https://doi.org/10.1016/j.palaeo.2020.109956

Wilhelm, M., & Bloom, N. (2000). Mercury in petroleum. *Fuel Processing Technology*, *63*(1), 1–27. https://doi.org/10.1016/S0378-3820(99)00068-5

Wilhelm, S. M. (2001). Estimate of mercury emissions to the atmosphere from petroleum. *Environmental Science and Technology*, *35*(24), 4704–4710. https://doi.org/10.1021/es001804h

Wilkes, H., Disko, U., & Horsfield, B. (1998). Aromatic aldehydes and ketones in the Posidonia Shale, Hils Syncline, Germany. *Organic Geochemistry*, *29*(1–3), 107–117. https://doi.org/10.1016/S0146-6380(98)00138-7

Zaferani, S., Pérez-rodríguez, M., & Biester, H. (2018). Diatom ooze—A large marine mercury sink. *Science, 361*(6404), 797-800. https://doi.org/10.1016/j.

scitotenv.2020.143940